

Supplementary document for “Simultaneous multiple
change-point and factor analysis for high-dimensional time
series”

February 1, 2018

This document reports additional results from the simulation studies conducted in Section 7 of Barigozzi et al. (2018) (Sections 1 and 3), and comparative simulation studies conducted with the methods proposed in Han and Inoue (2014) and Chen et al. (2014) (Section 2).

1 Single change-point detection

We report further results from the simulation study conducted in Section 7.1 of Barigozzi et al. (2018).

1.1 When $n = 100$

1.1.1 Estimated change-point locations

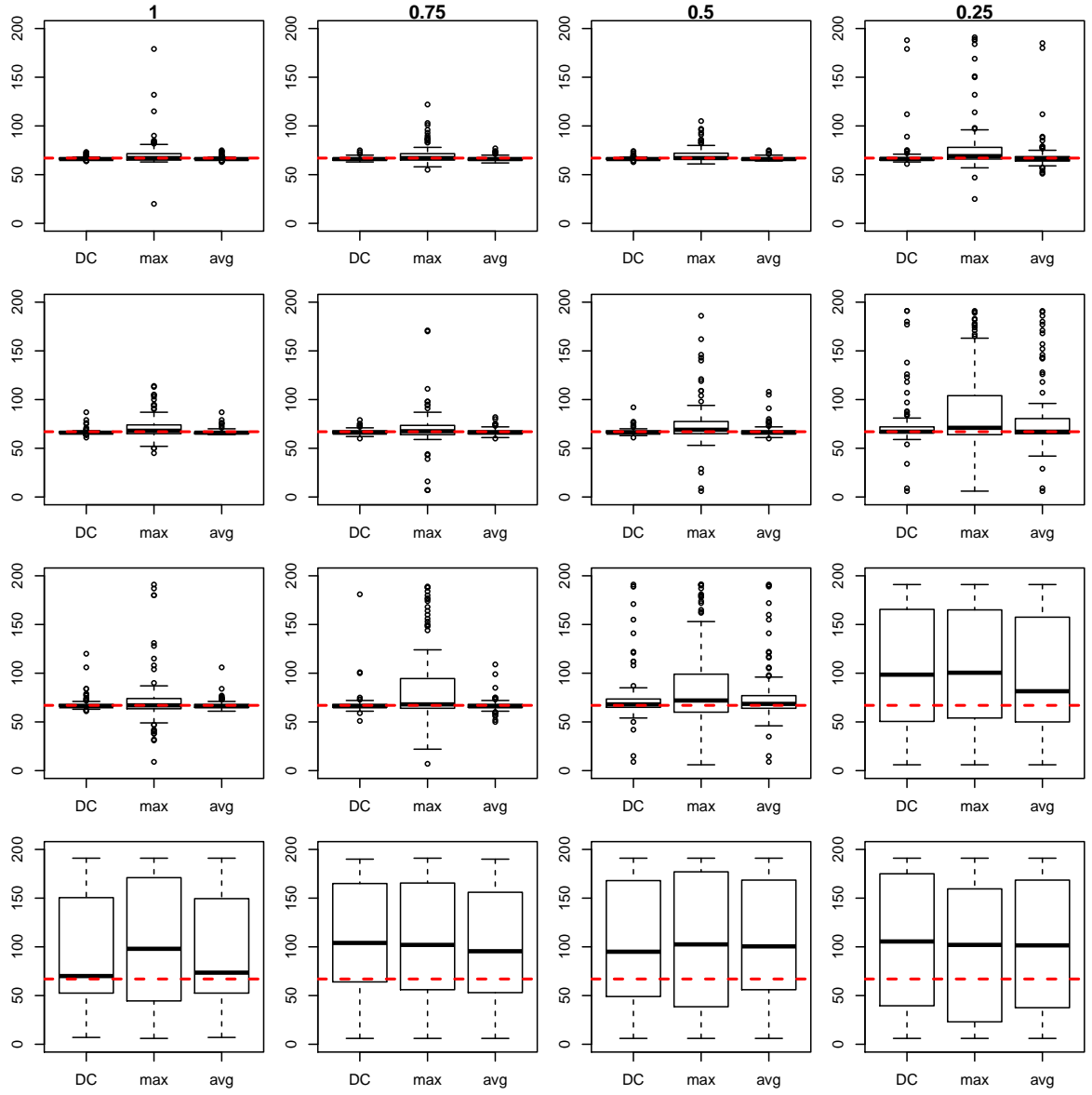


Figure 1: (S1) BOXPLOTS OF THE LOCATIONS OF CHANGE-POINTS ESTIMATED FROM $\hat{\chi}_{it}^*$ FOR $\sigma \in \sqrt{2}\{1, 0.75, 0.5, 0.25\}$ (TOP TO BOTTOM) AND $\rho \in \{1, 0.75, 0.5, 0.25\}$ (LEFT TO RIGHT), WHEN $n = 100$, $T = 200$ AND $\phi = 1$; HORIZONTAL BROKEN LINES INDICATE THE TRUE CHANGE-POINT LOCATION $\eta = [T/3]$.

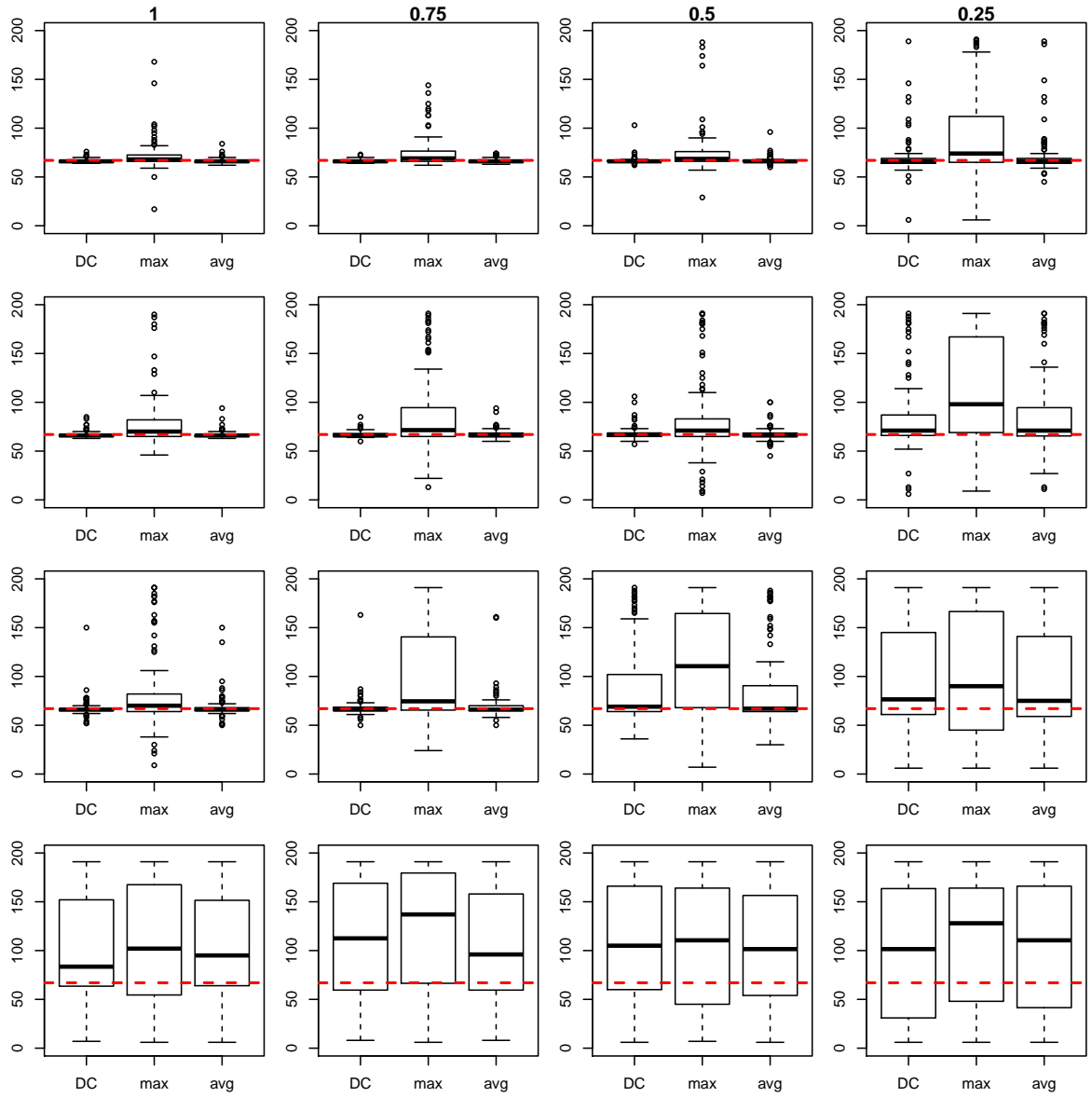


Figure 2: (S1) BOXPLOTS OF THE LOCATIONS OF CHANGE-POINTS ESTIMATED FROM $\hat{\chi}_{it}^*$ WHEN $n = 100$, $T = 200$ AND $\phi = 1.5$.

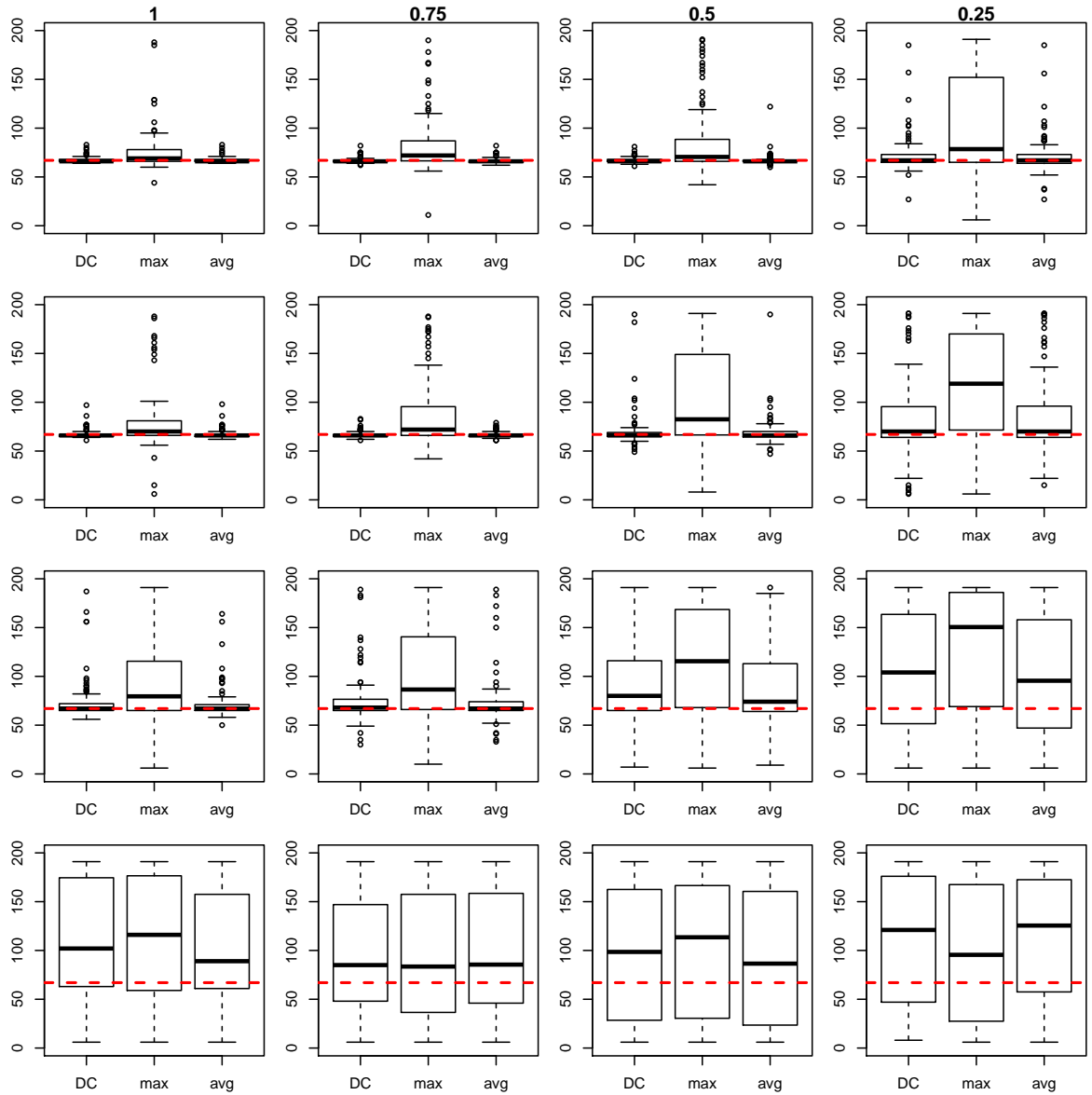


Figure 3: (S1) BOXPLOTS OF THE LOCATIONS OF CHANGE-POINTS ESTIMATED FROM $\hat{\chi}_{it}^*$ WHEN $n = 100$, $T = 200$ AND $\phi = 2$.

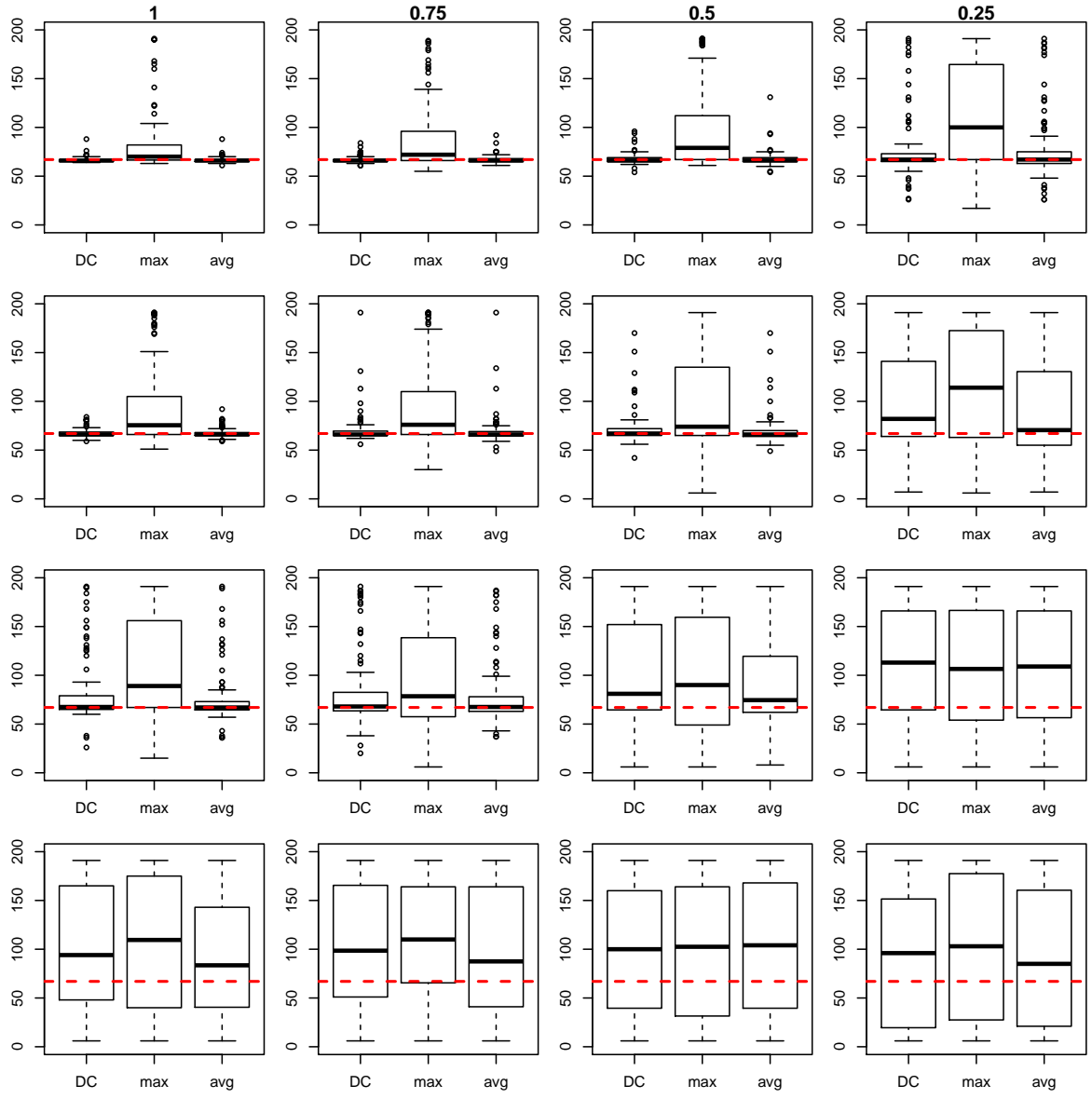


Figure 4: (S1) BOXPLOTS OF THE LOCATIONS OF CHANGE-POINTS ESTIMATED FROM $\hat{\chi}_{it}^*$ WHEN $n = 100$, $T = 200$ AND $\phi = 2.5$.

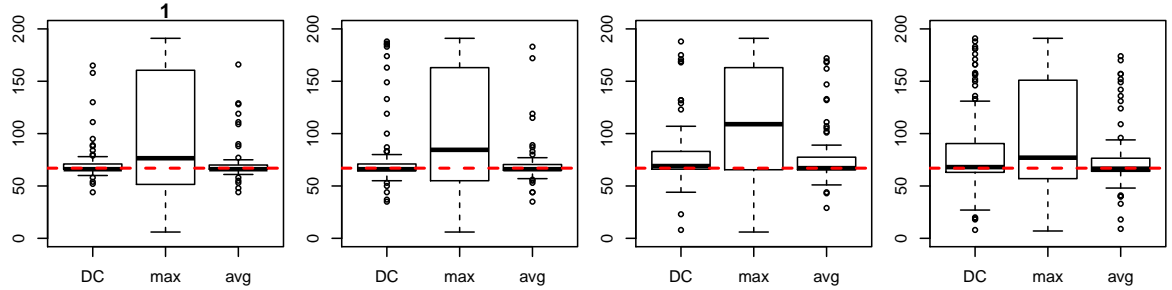


Figure 5: (S2) BOXPLOTS OF THE LOCATIONS OF CHANGE-POINTS ESTIMATED FROM $\hat{\chi}_{it}^*$ FOR $\phi \in \{1, 1.5, 2, 2.5\}$ (LEFT TO RIGHT), WHEN $n = 100$ AND $T = 200$.

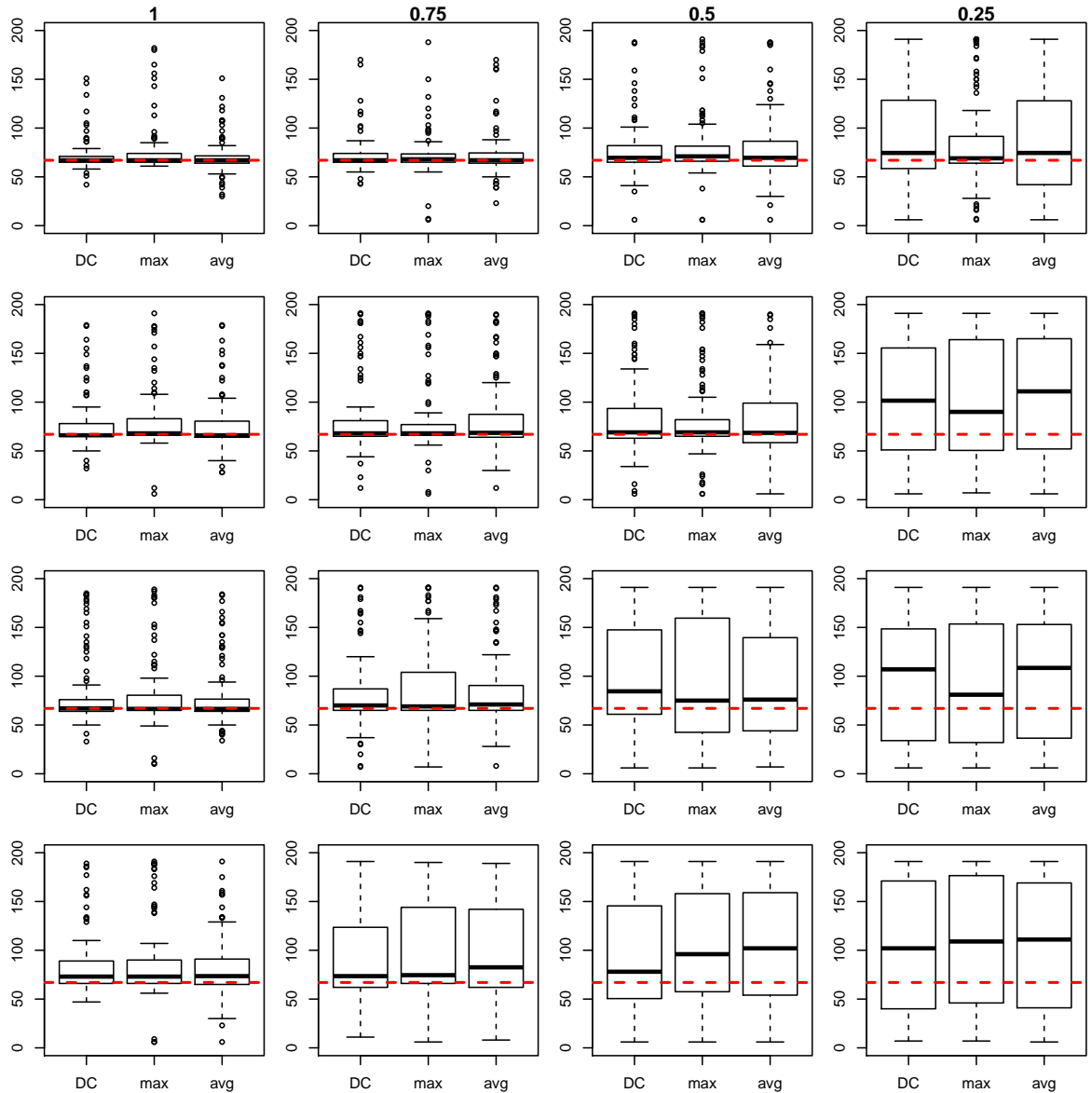


Figure 6: (S3) BOXPLOTS OF THE LOCATIONS OF CHANGE-POINTS ESTIMATED FROM $\widehat{\chi}_{it}^*$ FOR $\phi \in \{1, 1.5, 2, 2.5\}$ (TOP TO BOTTOM) AND $\varrho \in \{1, 0.75, 0.5, 0.25\}$ (LEFT TO RIGHT), WHEN $n = 100$, $T = 200$.

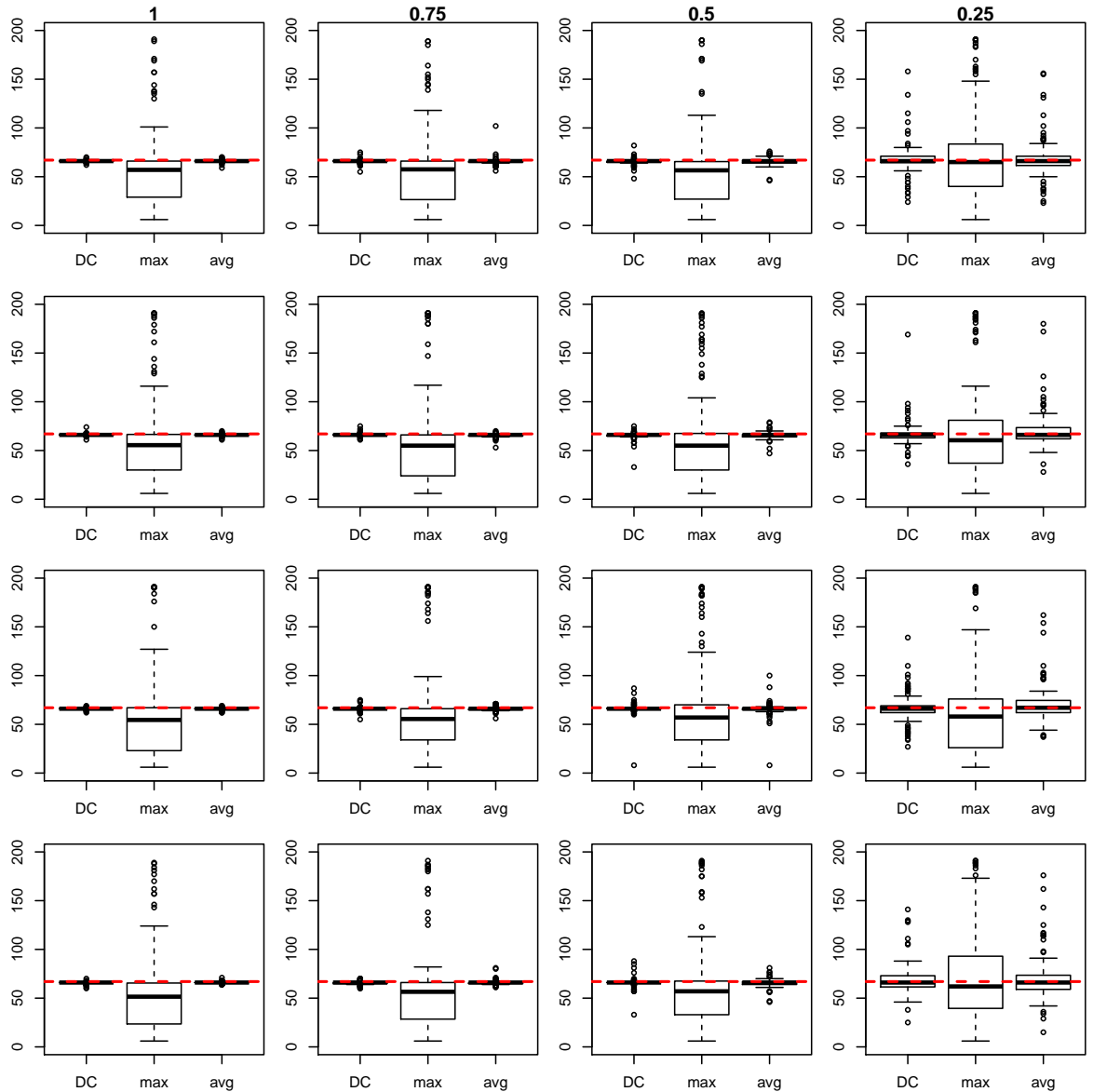


Figure 7: (S4) BOXPLOTS OF THE LOCATIONS OF CHANGE-POINTS ESTIMATED FROM $\hat{\epsilon}_{it}^*$ FOR $\phi^{-1} \in \{1, 1.5, 2, 2.5\}$ (TOP TO BOTTOM) AND $\varrho \in \{1, 0.75, 0.5, 0.25\}$ (LEFT TO RIGHT), WHEN $n = 100$ AND $T = 200$.

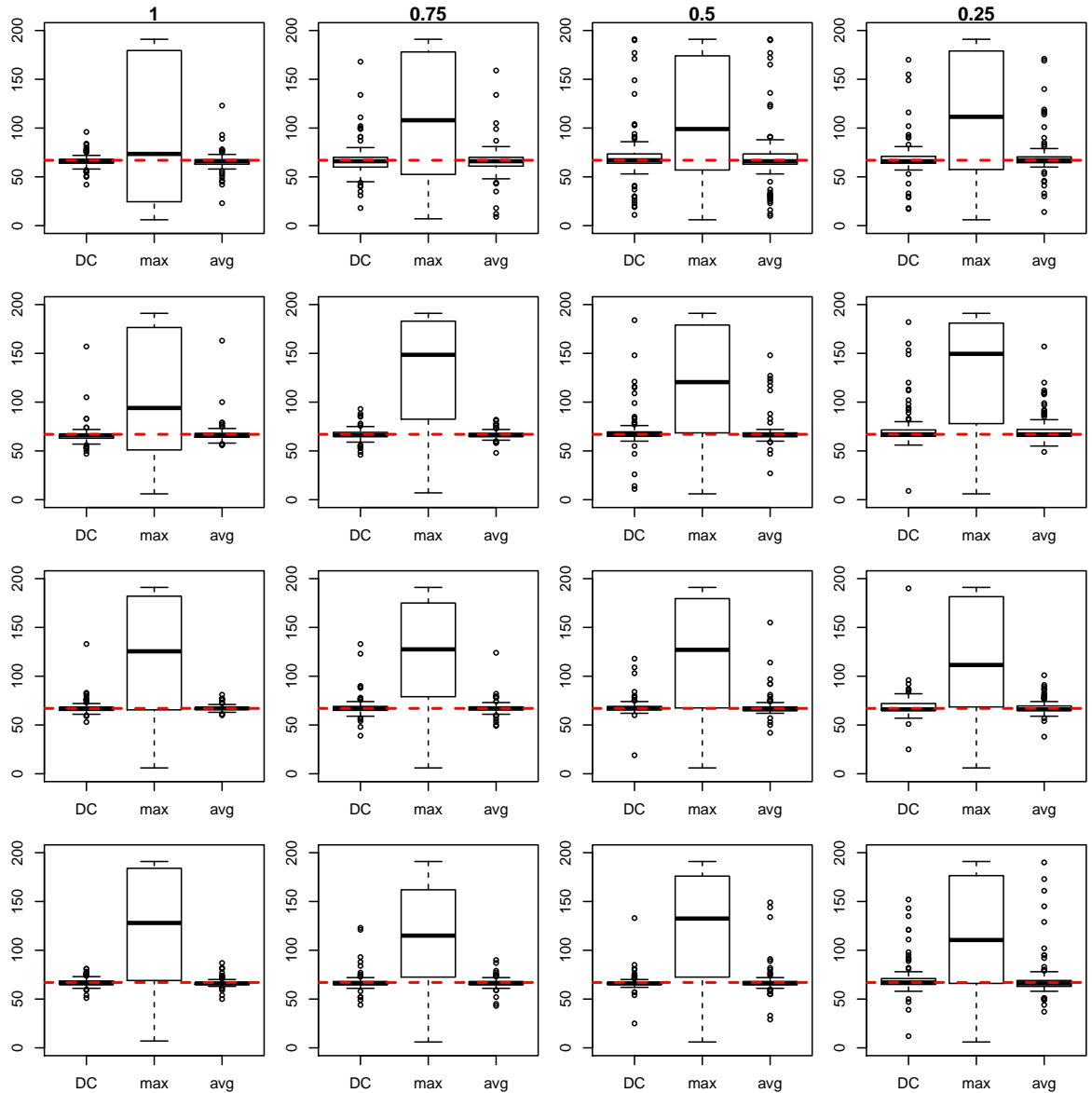


Figure 8: (S5) BOXPLOTS OF THE LOCATIONS OF CHANGE-POINTS ESTIMATED FROM $\hat{\epsilon}_{it}^*$ FOR $\phi^{-1} \in \{1, 1.5, 2, 2.5\}$ (TOP TO BOTTOM) AND $\varrho \in \{1, 0.75, 0.5, 0.25\}$ (LEFT TO RIGHT), WHEN $n = 100$ AND $T = 200$.

Table 8: (S5) SUMMARY OF CHANGE-POINT ANALYSIS WHEN $n = 100$ AND $T = 200$.

ϕ^{-1}	ϱ	1			0.75			0.5			0.25			
		DC	max	avg	DC	max	avg	DC	max	avg	DC	max	avg	
1	$\hat{\chi}_{it}^*$	avg($\hat{\eta}_1$)	66.96	89.39	66.20	68.05	94.96	67.44	82.78	103.85	87.68	91.43	93.37	92.07
		sd($\hat{\eta}_1$)	5.28	37.03	5.87	11.08	42.43	12.32	43.17	60.93	50.06	61.61	65.32	61.39
		power	1.00	0.78	1.00	0.99	0.58	0.98	0.69	0.32	0.62	0.22	0.19	0.21
	$\hat{\epsilon}_{it}^*$	avg($\hat{\eta}_1$)	66.32	97.35	65.68	67.58	109.88	65.36	71.27	106.31	69.92	69.24	107.94	70.76
		sd($\hat{\eta}_1$)	6.76	72.56	9.94	18.55	65.86	17.67	30.07	66.83	32.28	20.55	68.59	21.57
		power	0.94	0.15	0.90	0.75	0.11	0.64	0.53	0.05	0.45	0.78	0.11	0.76
1.5	$\hat{\chi}_{it}^*$	avg($\hat{\eta}_1$)	84.33	101.43	79.24	89.66	102.67	86.31	101.21	101.01	96.81	95.26	96.36	99.78
		sd($\hat{\eta}_1$)	43.26	48.19	44.41	53.42	53.21	53.12	62.93	60.69	63.65	62.50	62.86	60.24
		power	0.64	0.32	0.58	0.30	0.23	0.28	0.24	0.13	0.19	0.10	0.10	0.06
	$\hat{\epsilon}_{it}^*$	avg($\hat{\eta}_1$)	66.13	105.99	67.32	66.94	130.68	66.69	70.23	119.47	69.62	74.06	127.40	71.96
		sd($\hat{\eta}_1$)	11.31	67.14	11.12	6.72	55.73	4.42	20.06	59.24	15.52	22.09	59.39	15.14
		power	0.94	0.09	0.91	0.93	0.06	0.92	0.81	0.12	0.85	0.89	0.07	0.82
2	$\hat{\chi}_{it}^*$	avg($\hat{\eta}_1$)	89.99	106.88	84.44	88.14	100.76	84.68	95.20	90.00	96.85	91.10	104.76	87.25
		sd($\hat{\eta}_1$)	57.12	54.00	53.13	59.97	62.17	60.52	56.43	61.84	55.58	64.95	65.35	63.91
		power	0.18	0.17	0.19	0.15	0.06	0.11	0.09	0.08	0.09	0.07	0.05	0.01
	$\hat{\epsilon}_{it}^*$	avg($\hat{\eta}_1$)	67.82	115.14	67.29	68.42	122.49	67.46	68.53	118.65	68.53	69.75	114.19	68.09
		sd($\hat{\eta}_1$)	7.86	66.79	3.25	10.74	58.17	7.60	9.76	63.89	11.97	14.79	61.21	7.75
		power	0.98	0.07	1.00	0.95	0.09	0.93	0.92	0.07	0.91	0.83	0.02	0.76
2.5	$\hat{\chi}_{it}^*$	avg($\hat{\eta}_1$)	92.22	110.91	88.89	96.79	92.59	100.88	96.28	92.34	93.13	96.33	95.30	94.01
		sd($\hat{\eta}_1$)	58.56	60.14	57.41	67.68	59.30	66.07	65.81	64.78	67.45	64.49	65.57	62.66
		power	0.11	0.18	0.08	0.10	0.05	0.09	0.07	0.07	0.08	0.11	0.05	0.07
	$\hat{\epsilon}_{it}^*$	avg($\hat{\eta}_1$)	67.16	121.06	66.68	67.80	111.56	66.43	67.16	119.45	68.28	71.64	114.08	71.11
		sd($\hat{\eta}_1$)	4.46	62.78	4.43	9.78	56.93	5.73	8.90	59.74	15.02	18.32	62.06	22.89
		power	0.98	0.06	0.97	0.97	0.09	0.95	0.94	0.04	0.95	0.82	0.05	0.78

1.2 When $n = 300$

1.2.1 Detection power

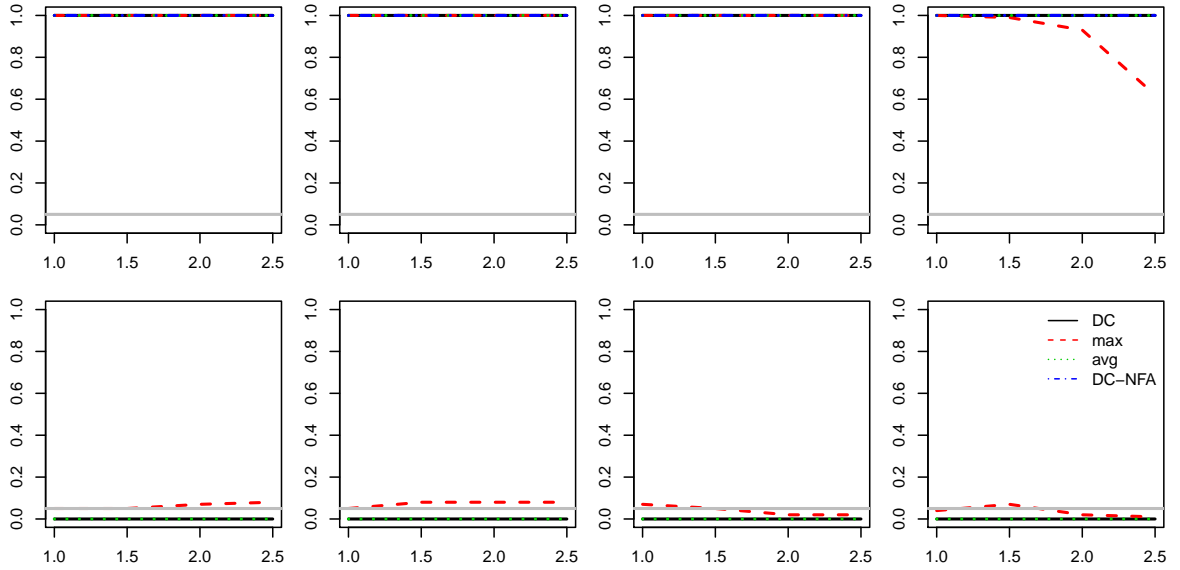


Figure 9: (S1) DETECTION POWER (y -AXIS) OF CHANGE-POINT TESTS BASED ON DC (SOLID), MAX (BROKEN) AND AVG (DOTTED) ON THE COMMON (TOP) AND IDIOSYNCRATIC (BOTTOM) COMPONENTS WITH VARYING $\phi \in \{1, 1.5, 2, 2.5\}$ (x -AXIS) WHEN $n = 300$, $T = 200$, $\sigma = \sqrt{2}$ AND $\varrho \in \{1, 0.75, 0.5, 0.25\}$ (LEFT TO RIGHT); HORIZONTAL GREY LINES INDICATE THE SIGNIFICANCE LEVEL 0.05.

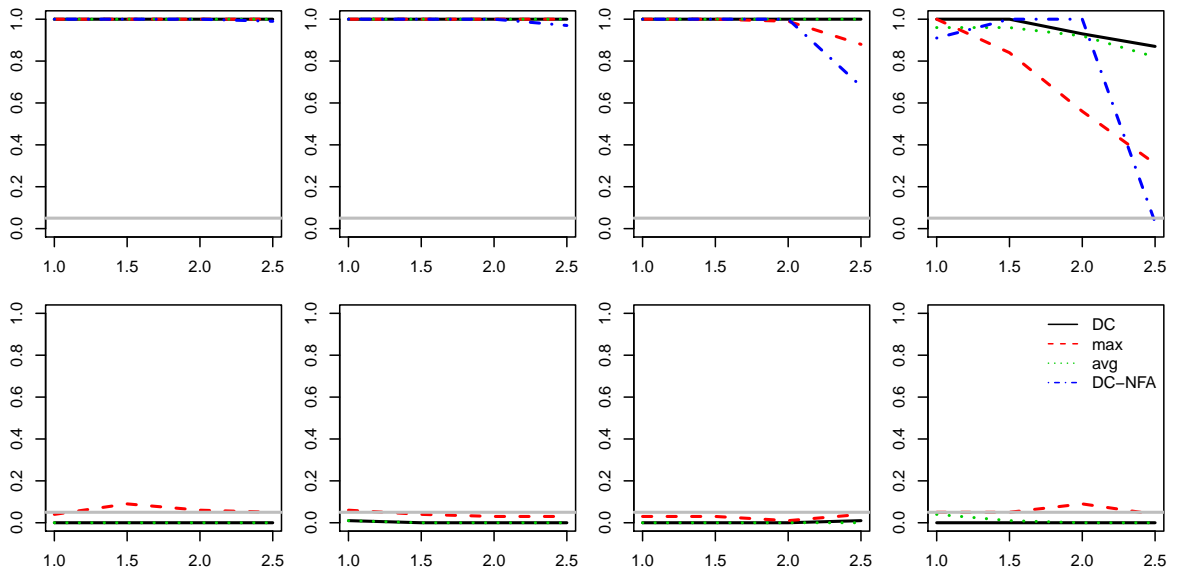


Figure 10: (S1) DETECTION POWER OF CHANGE-POINT TESTS WHEN $\sigma = 0.75\sqrt{2}$.

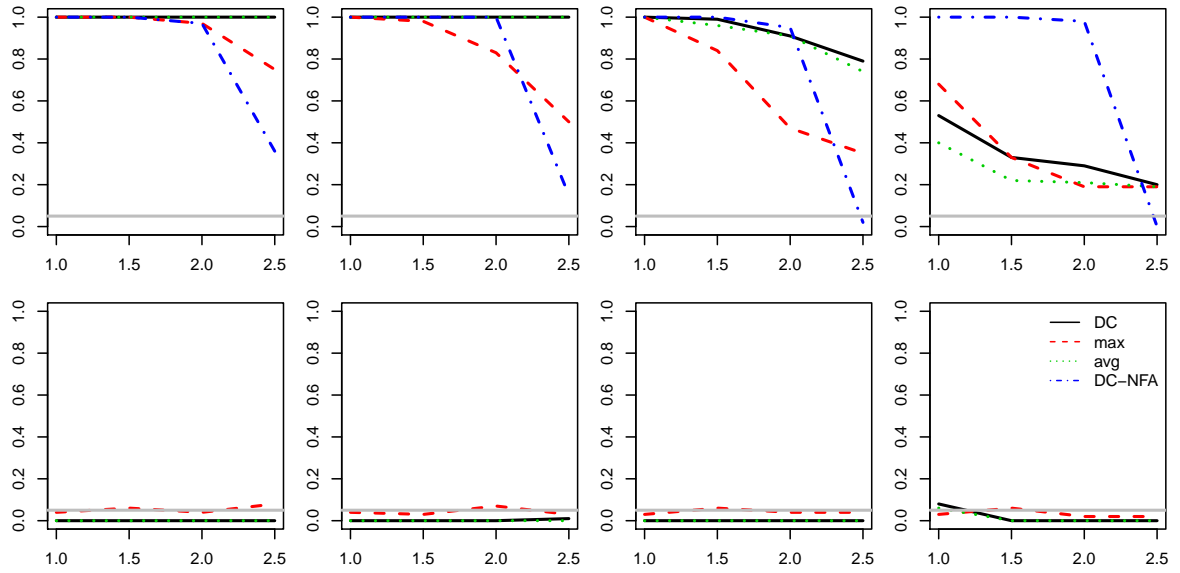


Figure 11: (S1) DETECTION POWER OF CHANGE-POINT TESTS WHEN $\sigma = 0.5\sqrt{2}$.

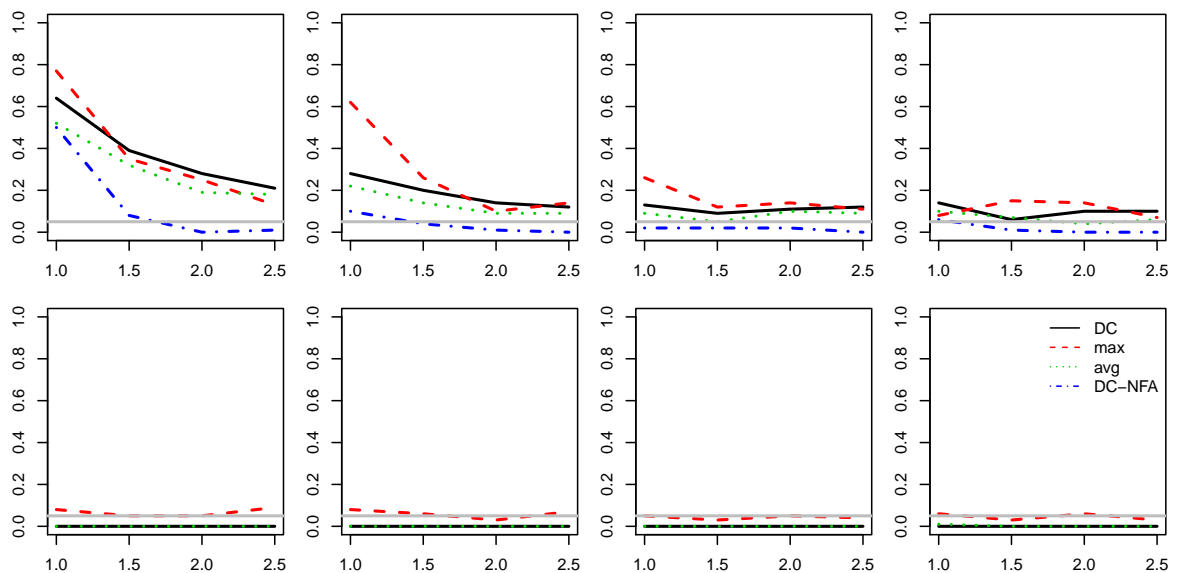


Figure 12: (S1) DETECTION POWER OF CHANGE-POINT TESTS WHEN $\sigma = 0.25\sqrt{2}$.

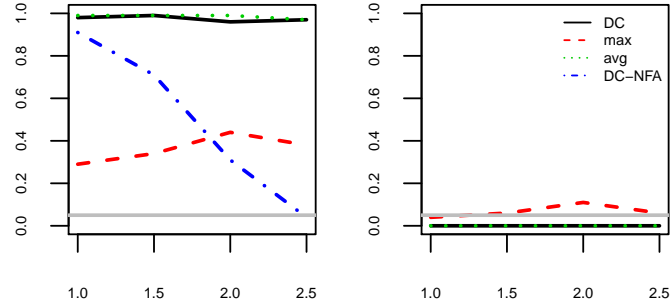


Figure 13: (S2) DETECTION POWER OF CHANGE-POINT TESTS ON THE COMMON (LEFT) AND IDIOSYNCRATIC (RIGHT) COMPONENTS WITH VARYING $\phi \in \{1, 1.5, 2, 2.5\}$ (x -AXIS) WHEN $n = 300$ AND $T = 200$.

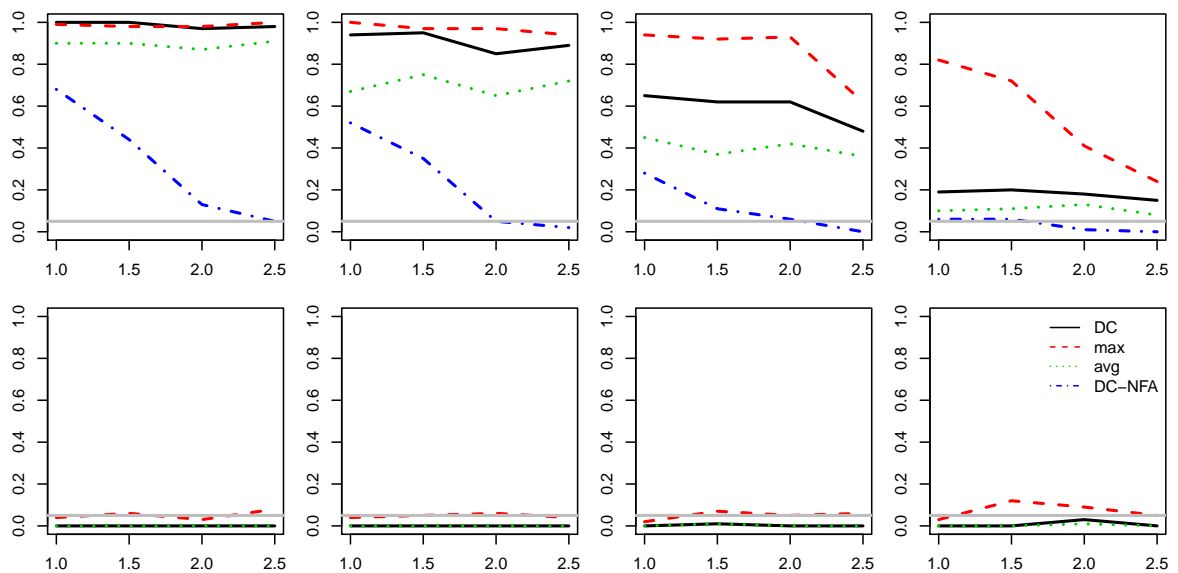


Figure 14: (S3) DETECTION POWER OF CHANGE-POINT TESTS ON THE COMMON (TOP) AND IDIOSYNCRATIC (BOTTOM) COMPONENTS WITH VARYING $\phi \in \{1, 1.5, 2, 2.5\}$ (x -AXIS) WHEN $n = 300$, $T = 200$, $\sigma = \sqrt{2}$ AND $\rho \in \{1, 0.75, 0.5, 0.25\}$ (LEFT TO RIGHT).

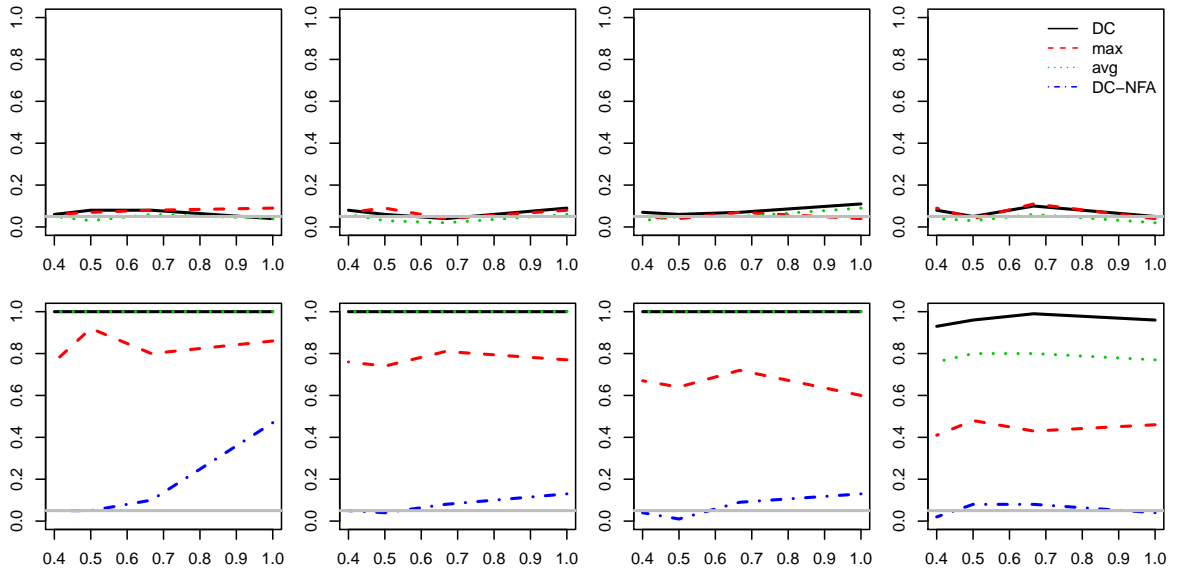


Figure 15: (S4) DETECTION POWER OF CHANGE-POINT TESTS ON THE COMMON (TOP) AND IDIOSYNCRATIC (BOTTOM) COMPONENTS WITH VARYING $\phi \in \{2.5^{-1}, 2^{-1}, 1.5^{-1}, 1\}$ (x -axis) WHEN $n = 300$, $T = 200$ AND $\varrho \in \{1, 0.75, 0.5, 0.25\}$ (LEFT TO RIGHT).

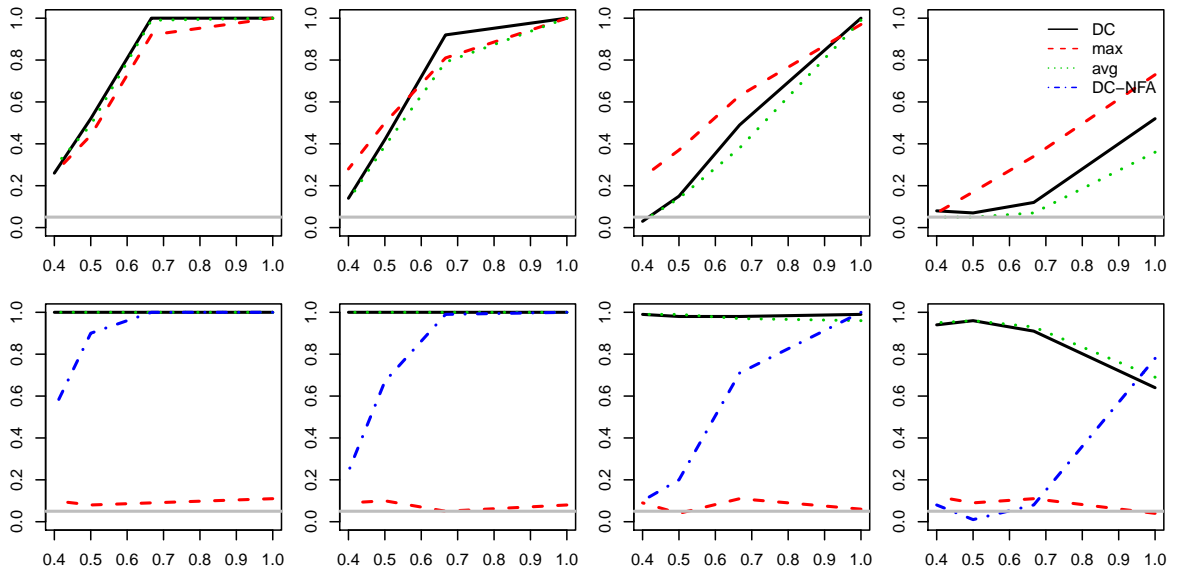


Figure 16: (S5) DETECTION POWER OF CHANGE-POINT TESTS ON THE COMMON (TOP) AND IDIOSYNCRATIC (BOTTOM) COMPONENTS WITH VARYING $\phi \in \{2.5^{-1}, 2^{-1}, 1.5^{-1}, 1\}$ (x -axis) WHEN $n = 300$, $T = 200$ AND $\varrho \in \{1, 0.75, 0.5, 0.25\}$ (LEFT TO RIGHT).

1.2.2 Estimated change-point locations

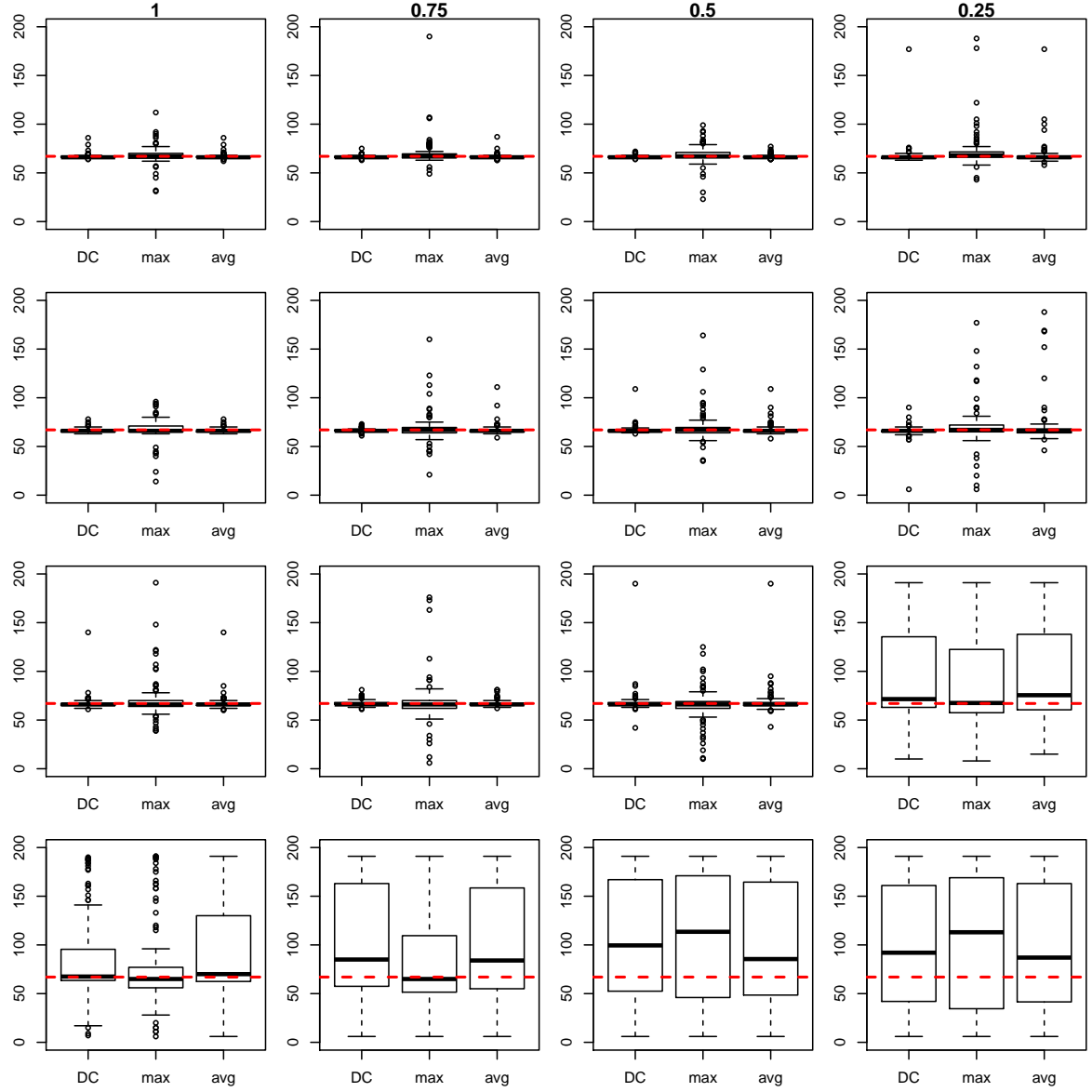


Figure 17: (S1) BOXPLOTS OF THE LOCATIONS OF CHANGE-POINTS ESTIMATED FROM $\widehat{\chi}_{it}^*$ FOR $\sigma \in \sqrt{2}\{1, 0.75, 0.5, 0.25\}$ (TOP TO BOTTOM) AND $\rho \in \{1, 0.75, 0.5, 0.25\}$ (LEFT TO RIGHT), WHEN $n = 300$, $T = 200$ AND $\phi = 1$; HORIZONTAL BROKEN LINES INDICATE THE TRUE CHANGE-POINT LOCATION $\eta = [T/3]$.

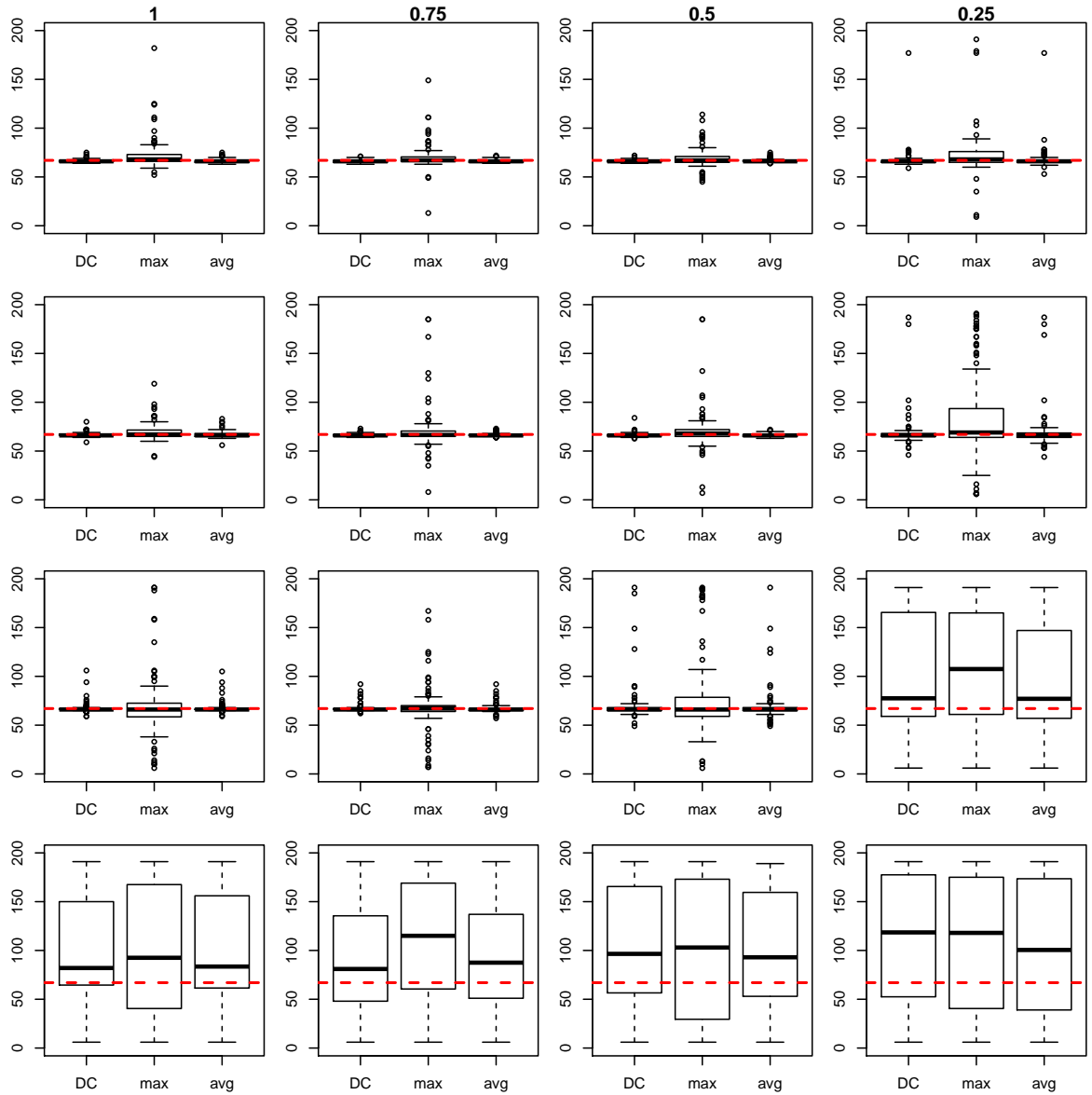


Figure 18: (S1) BOXPLOTS OF THE LOCATIONS OF CHANGE-POINTS ESTIMATED FROM $\hat{\chi}_{it}^*$ WHEN $n = 300$, $T = 200$ AND $\phi = 1.5$.

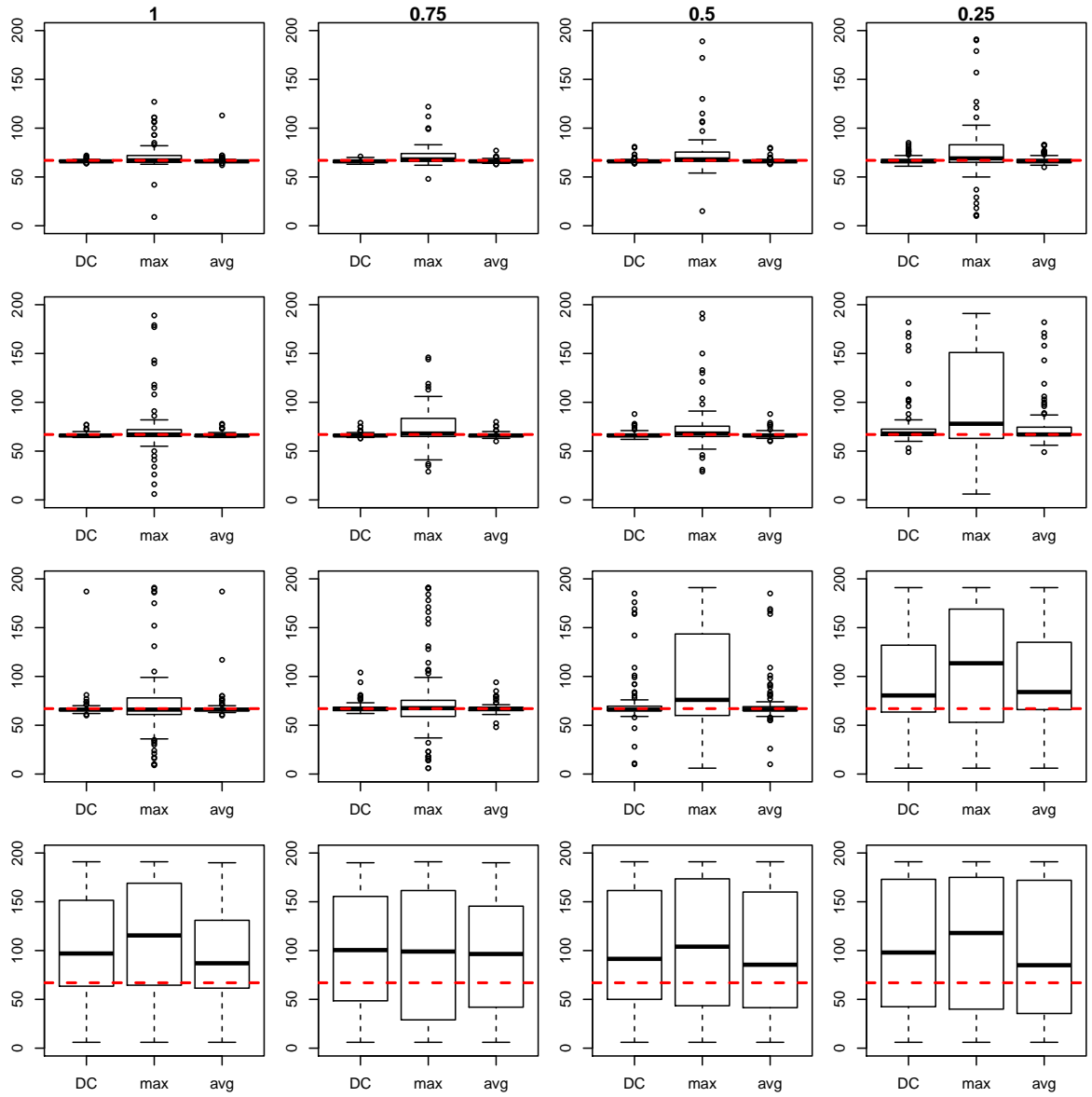


Figure 19: (S1) BOXPLOTS OF THE LOCATIONS OF CHANGE-POINTS ESTIMATED FROM $\hat{\chi}_{it}^*$ WHEN $n = 300$, $T = 200$ AND $\phi = 2$.

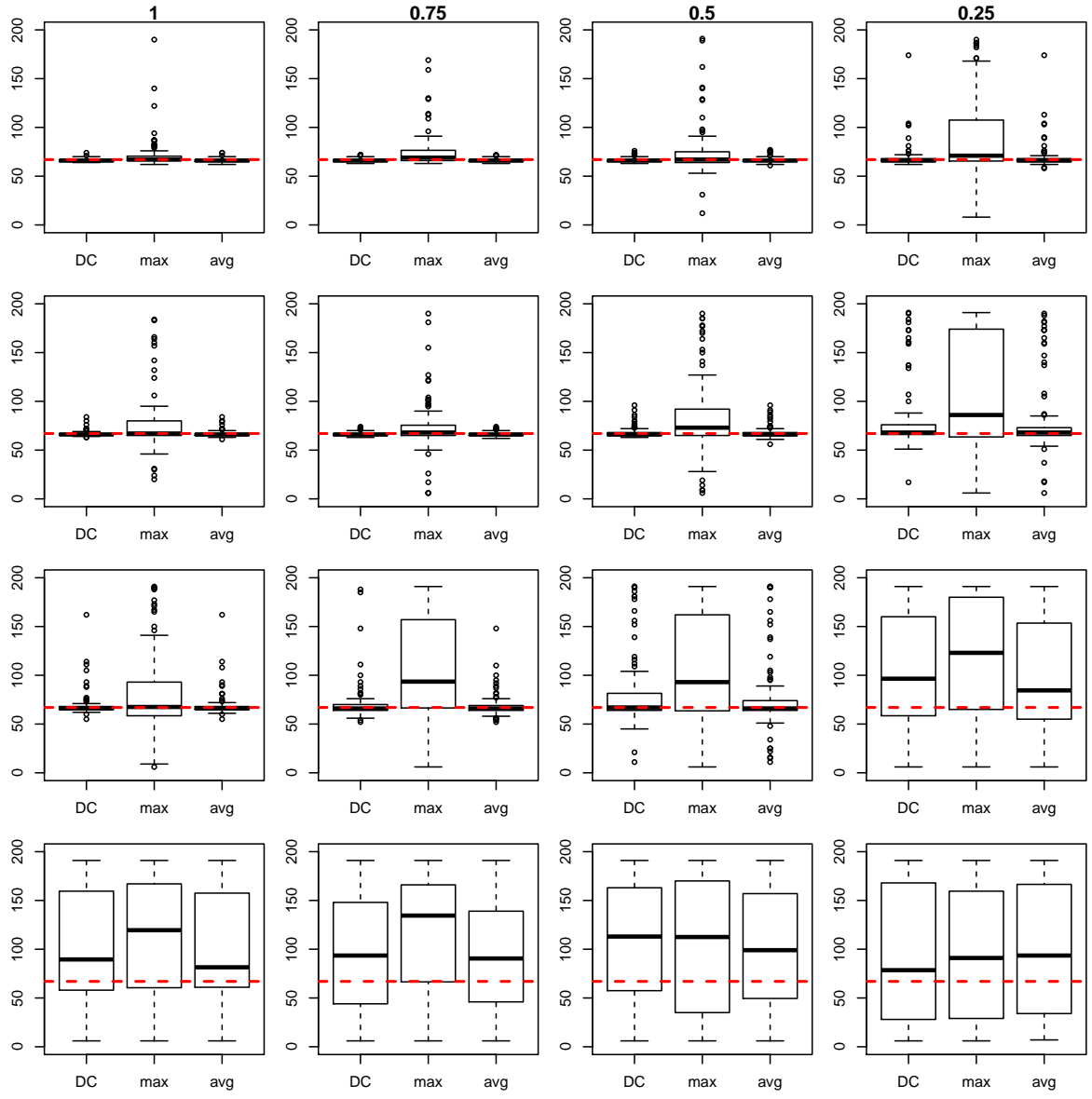


Figure 20: (S1) BOXPLOTS OF THE LOCATIONS OF CHANGE-POINTS ESTIMATED FROM $\hat{\chi}_{it}^*$ WHEN $n = 300$, $T = 200$ AND $\phi = 2.5$.

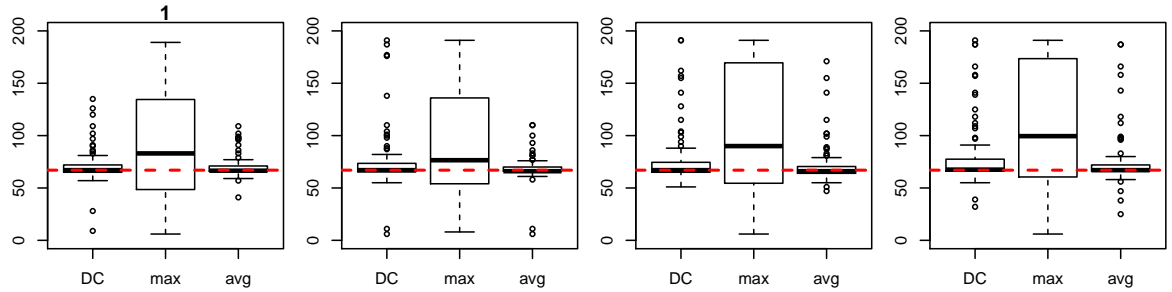


Figure 21: (S2) BOXPLOTS OF THE LOCATIONS OF CHANGE-POINTS ESTIMATED FROM $\hat{\chi}_{it}^*$ FOR $\phi \in \{1, 1.5, 2, 2.5\}$ (LEFT TO RIGHT), WHEN $n = 300$ AND $T = 200$.

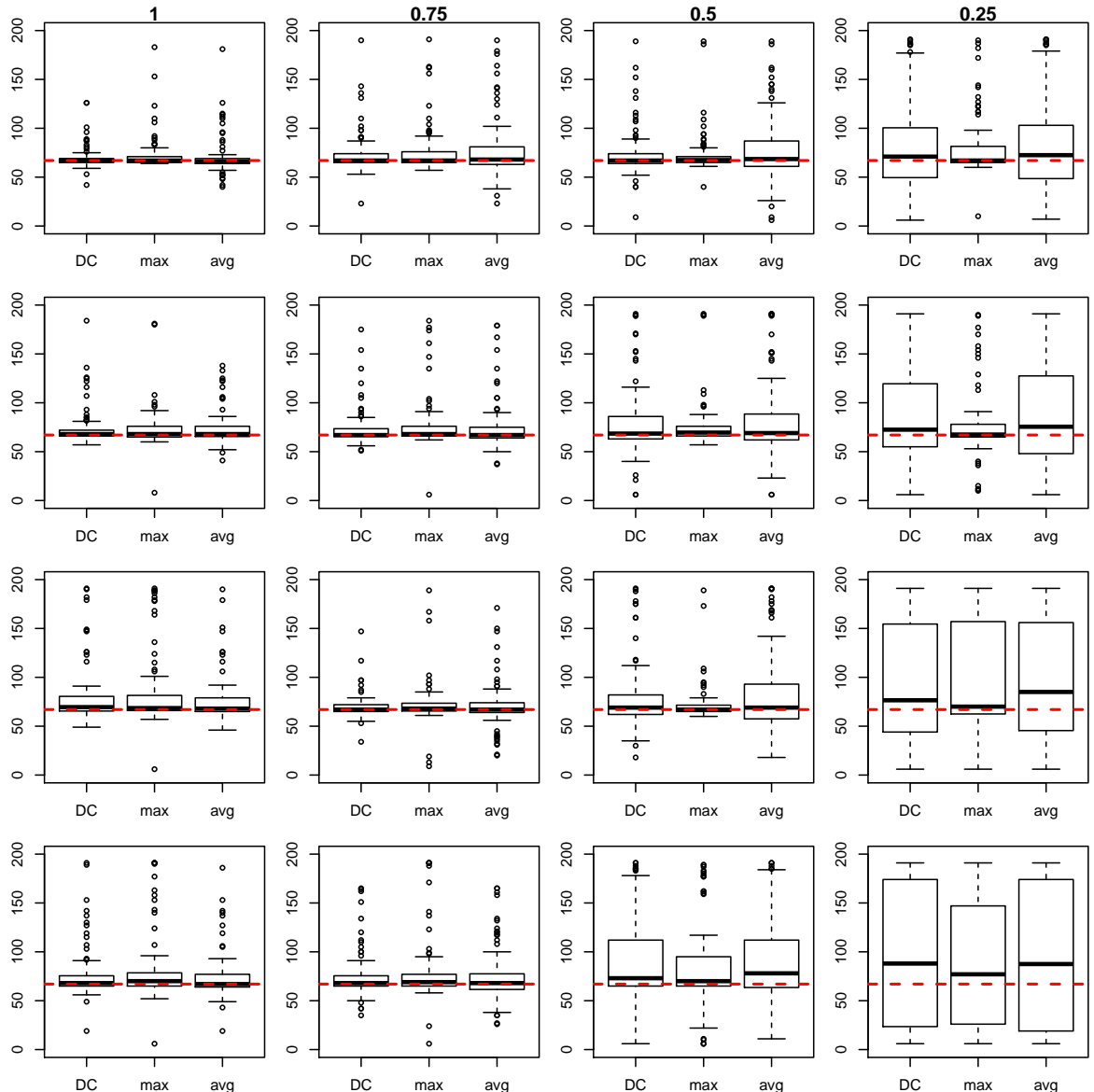


Figure 22: (S3) BOXPLOTS OF THE LOCATIONS OF CHANGE-POINTS ESTIMATED FROM $\hat{\chi}_{it}^*$ FOR $\phi \in \{1, 1.5, 2, 2.5\}$ (TOP TO BOTTOM) AND $\varrho \in \{1, 0.75, 0.5, 0.25\}$ (LEFT TO RIGHT), WHEN $n = 300$, $T = 200$.

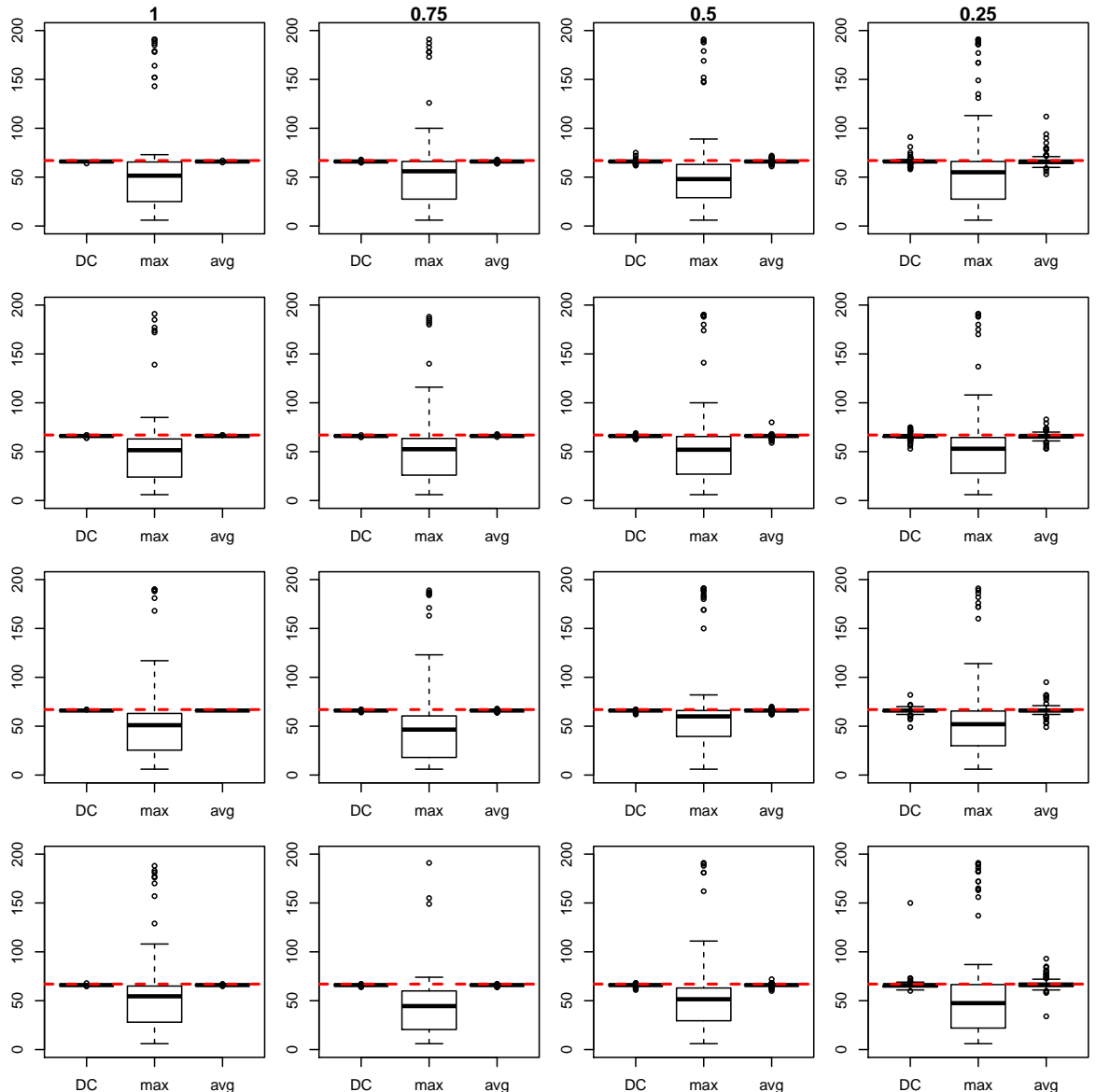


Figure 23: (S4) BOXPLOTS OF THE LOCATIONS OF CHANGE-POINTS ESTIMATED FROM $\hat{\epsilon}_{it}^*$ FOR $\phi^{-1} \in \{1, 1.5, 2, 2.5\}$ (TOP TO BOTTOM) AND $\varrho \in \{1, 0.75, 0.5, 0.25\}$ (LEFT TO RIGHT), WHEN $n = 300$ AND $T = 200$.

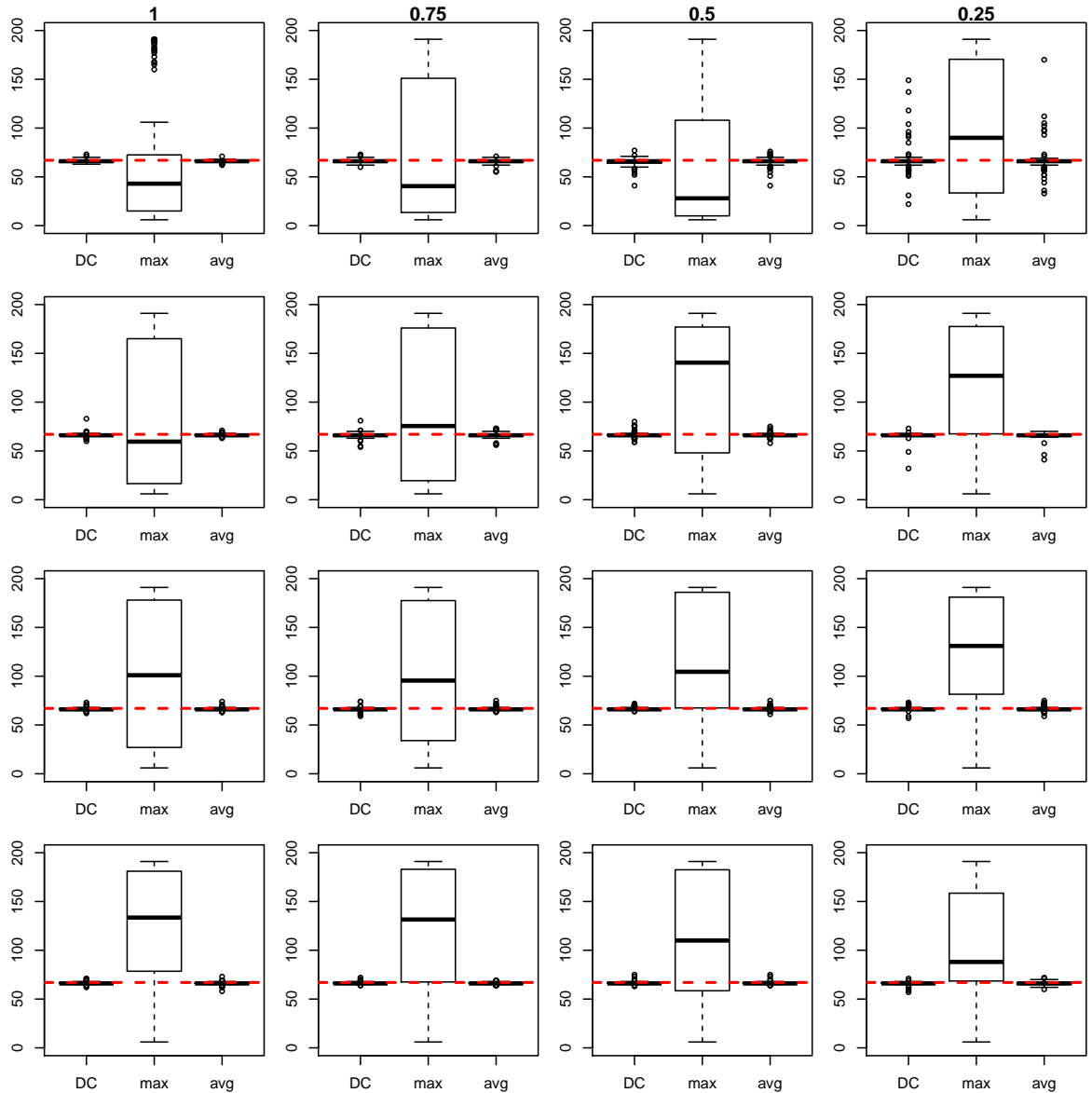


Figure 24: (S5) BOXPLOTS OF THE LOCATIONS OF CHANGE-POINTS ESTIMATED FROM $\hat{\epsilon}_{it}^*$ FOR $\phi^{-1} \in \{1, 1.5, 2, 2.5\}$ (TOP TO BOTTOM) AND $\rho \in \{1, 0.75, 0.5, 0.25\}$ (LEFT TO RIGHT), WHEN $n = 300$ AND $T = 200$.

Table 16: (S5) SUMMARY OF CHANGE-POINT ANALYSIS WHEN $n = 300$ AND $T = 200$.

ϕ^{-1}	ϱ	1			0.75			0.5			0.25			
		DC	max	avg	DC	max	avg	DC	max	avg	DC	max	avg	
1	$\hat{\chi}_{it}^*$	avg($\hat{\eta}_1$)	66.04	80.92	65.49	66.19	77.86	65.54	66.36	82.47	66.17	82.99	85.42	87.96
		sd($\hat{\eta}_1$)	1.87	26.54	3.90	1.72	21.50	3.44	3.70	28.83	6.23	55.10	51.79	59.94
		power	1.00	1.00	1.00	1.00	1.00	1.00	1.00	0.97	0.99	0.52	0.73	0.36
	$\hat{\epsilon}_{it}^*$	avg($\hat{\eta}_1$)	66.09	65.80	65.96	66.15	74.64	65.83	65.24	65.13	65.46	67.98	96.18	67.44
		sd($\hat{\eta}_1$)	1.60	64.04	1.20	1.97	70.14	2.19	4.32	68.09	4.14	15.15	65.18	14.93
		power	1.00	0.11	1.00	1.00	0.08	1.00	0.99	0.06	0.96	0.64	0.04	0.69
1.5	$\hat{\chi}_{it}^*$	avg($\hat{\eta}_1$)	67.75	81.64	67.41	67.29	82.93	67.19	80.75	85.66	80.13	103.60	100.14	102.53
		sd($\hat{\eta}_1$)	9.81	27.50	12.94	20.57	32.73	24.31	42.93	32.72	43.61	62.05	54.14	63.43
		power	1.00	0.92	0.99	0.92	0.81	0.79	0.49	0.63	0.38	0.12	0.34	0.07
	$\hat{\epsilon}_{it}^*$	avg($\hat{\eta}_1$)	66.38	83.59	66.32	66.20	94.59	66.12	66.68	113.32	66.39	65.82	116.63	65.67
		sd($\hat{\eta}_1$)	2.22	71.94	1.24	2.80	71.98	2.47	3.00	68.51	1.90	3.96	63.14	3.52
		power	1.00	0.09	1.00	1.00	0.05	1.00	0.98	0.11	0.97	0.91	0.11	0.93
2	$\hat{\chi}_{it}^*$	avg($\hat{\eta}_1$)	83.42	95.24	79.15	89.36	98.41	86.55	88.29	99.92	84.85	107.72	109.21	105.97
		sd($\hat{\eta}_1$)	47.33	41.59	46.45	47.18	46.16	46.67	57.97	48.71	56.82	66.02	65.33	65.5
		power	0.52	0.44	0.49	0.42	0.50	0.39	0.15	0.37	0.14	0.07	0.17	0.05
	$\hat{\epsilon}_{it}^*$	avg($\hat{\eta}_1$)	66.41	102.53	66.48	66.42	102.25	66.46	66.76	112.77	66.68	66.36	128.26	66.5
		sd($\hat{\eta}_1$)	1.38	70.74	1.37	1.87	69.58	1.57	1.46	69.07	1.69	1.83	50.80	2.18
		power	1.00	0.08	1.00	1.00	0.10	1.00	0.98	0.04	0.99	0.96	0.09	0.96
2.5	$\hat{\chi}_{it}^*$	avg($\hat{\eta}_1$)	90.18	95.83	78.14	83.08	100.20	79.21	99.48	104.37	98.31	97.90	89.51	95.96
		sd($\hat{\eta}_1$)	52.30	43.66	49.16	53.84	49.75	55.09	57.71	53.92	57.71	67.29	64.86	65.11
		power	0.26	0.26	0.29	0.14	0.28	0.13	0.03	0.24	0.03	0.08	0.07	0.05
	$\hat{\epsilon}_{it}^*$	avg($\hat{\eta}_1$)	66.40	121.93	66.30	66.34	119.64	66.16	66.57	109.71	66.44	66.00	102.07	65.98
		sd($\hat{\eta}_1$)	1.33	62.38	1.62	1.13	66.11	1.14	1.52	67.36	1.54	1.68	56.01	1.71
		power	1.00	0.10	1.00	1.00	0.09	1.00	0.99	0.09	0.99	0.94	0.12	0.95

2 Comparative study with Chen et al. (2014) and Han and Inoue (2014)

In this section, we compare the size and power of the DC test (as defined in Section 7.1 of Barigozzi et al. (2018)), against sup-Wald and sup-LM (Lagrange Multiplier)-type tests proposed Chen et al. (2014) and Han and Inoue (2014). The test statistics from Han and Inoue (2014) compare the pre- and post-break covariance matrices of $\hat{\mathbf{f}} = (\hat{f}_{1t}, \dots, \hat{f}_{\hat{r}t})^\top$, while those from Chen et al. (2014) look for a structural break in the linear coefficients from regressing \hat{f}_{1t} onto $\hat{f}_{2t}, \dots, \hat{f}_{\hat{r}t}$, with \hat{r} estimated using the information criteria proposed in Bai and Ng (2002) in both papers. We refer to their Wald and LM-type tests by W_0 , W_B , LM_0 and LM_B , with the subscripts depending on the choice of sample variance estimates (0 stands for a conditional heteroscedasticity robust estimator and B for a heteroscedasticity and autocorrelation consistent estimator). Note that their methods are for testing the presence of a single change-point only, and the accuracy in change-point location estimation was not reported.

Among the various settings considered by Han and Inoue (2014), we select the most challenging ones. Even so, the choice of parameters in (S6)–(S9) below results in weaker cross-sectional correlations on the idiosyncratic components compared to (S1)–(S5) in Section 7.1 of Barigozzi et al. (2018).

Recall the factor model (12) of Barigozzi et al. (2018), where we set $n = T = 200$ and $q = 3$. Then we consider the following scenarios.

- (S6) $\lambda_{ij} \sim_{\text{iid}} \mathcal{N}(1/2, 1)$, $f_{jt} \sim_{\text{iid}} \mathcal{N}(0, 1)$, $\epsilon_{it} = \sigma_i(v_{it} + \beta \sum_{k=-H, k \neq 0}^H v_{i+k,t})$, $\sigma_i \sim_{\text{iid}} \mathcal{U}(0.5, 1.5)$, $v_{it} \sim_{\text{iid}} \mathcal{N}(0, 1)$ and $\vartheta = 15q/\{13(1 + 2H\beta^2)\}$.
- (S7) $f_{jt} = \rho_f f_{j,t-1} + u_{jt}$, $u_{jt} \sim_{\text{iid}} \mathcal{N}(0, 1 - \rho_f^2)$, $\epsilon_{it} = \sigma_i v_{it}$, $\sigma_i \sim_{\text{iid}} \mathcal{U}(0.5, 1.5)$, $v_{it} = \rho_v v_{i,t-1} + v_{it}$, $v_{it} \sim_{\text{iid}} \mathcal{N}(0, 1 - \rho_v^2)$ and $\vartheta = 15q/13$.
- (S8) $f_{jt}, \epsilon_{it} \sim_{\text{iid}} \mathcal{N}(0, 1)$, $\vartheta = (1 + b^2/4)q$, $\lambda_{ij} = \lambda_{ij}^0 \sim_{\text{iid}} \mathcal{N}(b/2, 1)$ for $t \leq T/2$ while $\lambda_{ij} = \lambda_{ij}^0 - b$ for $t \geq T/2 + 1$, where $b \in \{1/3, 2/3, 1, 2\}$.
- (S9) $f_{jt}, \epsilon_{it} \sim_{\text{iid}} \mathcal{N}(0, 1)$, $\vartheta = 5q/4$, $\lambda_{ij} = \lambda_{ij}^0 \sim_{\text{iid}} \mathcal{N}(1/2, 1)$ for $t \leq T/2$ while $\lambda_{ij} = c \cdot \lambda_{ij}^0$ for $t \geq T/2 + 1$, where $c^2 \in \{3/4, 1/2, 1/4, 0\}$.

The parameters are chosen as $\beta = 0.1$, $H = 6$, $\rho_f = 0.7$ and $\rho_v = 0.5$. (S6)–(S7) are designed to investigate the size behaviour of change-point tests. In (S6), both factors and idiosyncratic components are serially uncorrelated while ϵ_t is cross-sectionally correlated, whereas factors and idiosyncratic components are autocorrelated without any cross-sectional dependence in (S7). As can be seen from Table 17, the DC test is able to keep the size strictly below the nominal level ($\alpha = 0.05$) in both scenarios. Note that W_0 and LM_0 often reject the null hypothesis spuriously in the presence of serial correlations in factors and idiosyncratic components.

In (S8)–(S9), a single change-point occurs in the loadings at $t = T/2$. The magnitude of the change in loadings increases with increasing b in (S8), and with decreasing c in (S9). The DC test attains the best power in detecting the change-point for all scenarios while not returning any false alarm from $\hat{\epsilon}_{it}^*$. The contrast between our method and Wald or LM-type tests is most striking in (S8): when $b = 1/3$, the magnitude of the change is too small that $\hat{r} = 3$ is often returned by information criterion-based estimators. Hence, the power attained by these tests is comparable to the nominal level, whereas the DC test attains power close to 1 thanks to the screening procedure described in Section 4.3. The same observation applies to (S9) when $c = 3/4$. Although LM_0 and W_0 tests from Han and Inoue (2014) generally achieve higher power than the rest of Wald and LM-type tests, their poor size behaviour needs to be taken into account in interpreting their power.

Table 17: DETECTION POWER OF THE DC TEST AND CHANGE-POINT TESTS PROPOSED IN HAN AND INOUE (2014) AND CHEN ET AL. (2014) AT $\alpha = 0.05$ OVER 1000 REALISATIONS. THE RESULTS FROM THEIR WALD AND LM-TYPE TESTS ARE TAKEN FROM TABLES 1 AND 3A–3B OF HAN AND INOUE (2014); THEY DID NOT REPORT THE SIZE BEHAVIOUR OF THE TESTS PROPOSED BY CHEN ET AL. (2014).

b / c^2	DC		Han and Inoue (2014)				Chen et al. (2014)				
	$\hat{\chi}_{it}^*$	$\hat{\epsilon}_{it}^*$	W_0	W_B	LM_0	LM_B	W_0	W_B	LM_0	LM_B	
(S6) -	0.031	0.008	0.062	0.014	0.031	0.009	-	-	-	-	
(S7) -	0.029	0.000	0.852	0.061	0.840	0.050	-	-	-	-	
(S8)	1/3	0.963	0.003	0.078	0.022	0.065	0.023	0.070	0.059	0.048	0.029
	2/3	1.000	0.001	1.000	0.891	1.000	0.561	1.000	1.000	0.668	0.574
	1	1.000	0.004	1.000	0.919	1.000	0.614	1.000	1.000	0.778	0.663
	2	1.000	0.000	1.000	0.842	1.000	0.494	1.000	0.997	1.000	0.995
(S9)	3/4	0.345	0.000	0.202	0.056	0.194	0.061	0.048	0.044	0.039	0.028
	1/2	0.960	0.001	0.952	0.646	0.955	0.543	0.040	0.041	0.049	0.035
	1/4	1.000	0.001	1.000	0.983	1.000	0.759	0.023	0.035	0.056	0.043
	0	1.000	0.002	1.000	0.999	1.000	0.644	0.400	0.487	0.062	0.051

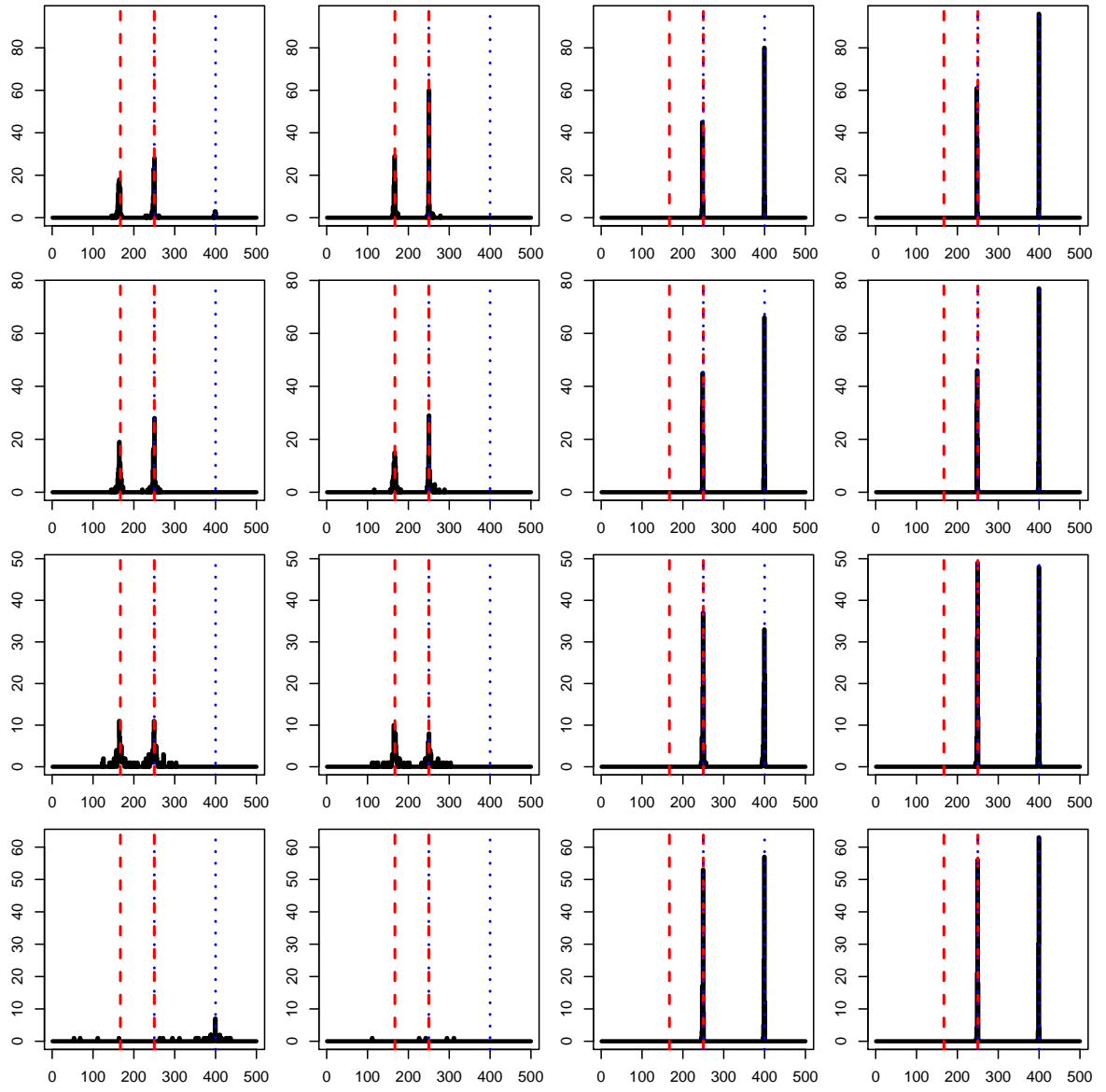


Figure 25: (M1) LOCATIONS OF THE CHANGE-POINTS ESTIMATED FROM $\hat{\chi}_{it}^*$, χ_{it} (ORACLE), $\hat{\epsilon}_{it}^*$ AND ϵ_{it} (ORACLE) BY THE DCBS ALGORITHM (LEFT TO RIGHT) FOR $\sigma \in \{1, 0.75, 0.5, 0.25\}$ (TOP TO BOTTOM) WHEN $n = 100$, $T = 500$ AND $\phi = 1.5$; VERTICAL LINES INDICATE THE LOCATIONS OF THE TRUE CHANGE-POINTS η_b^χ , $b = 1, 2$ (BROKEN) AND η_b^ϵ , $b = 1, 2$ (DOTTED).

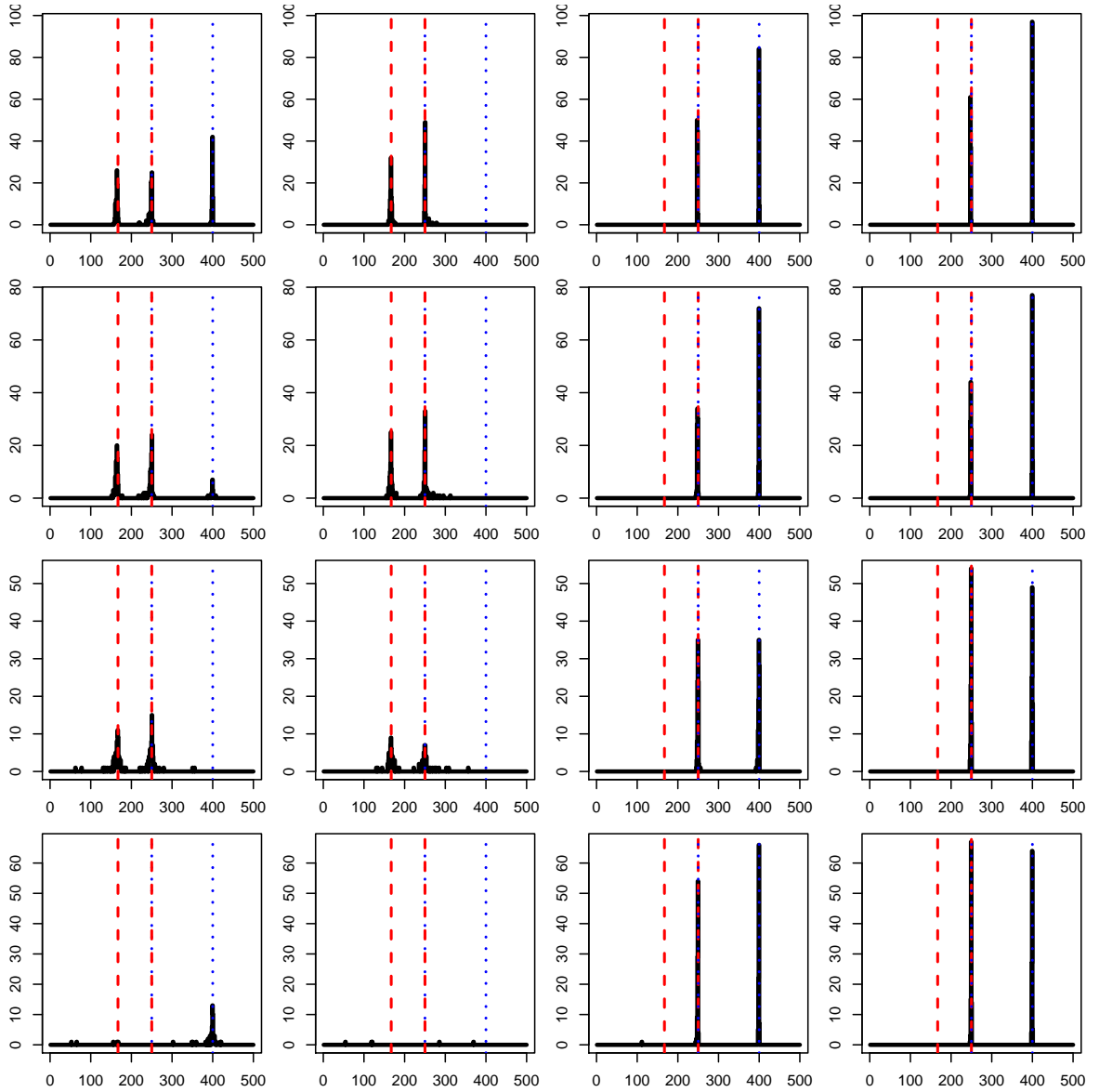


Figure 26: (M1) LOCATIONS OF THE ESTIMATED CHANGE-POINTS WHEN $n = 100$, $T = 500$ AND $\phi = 2$.

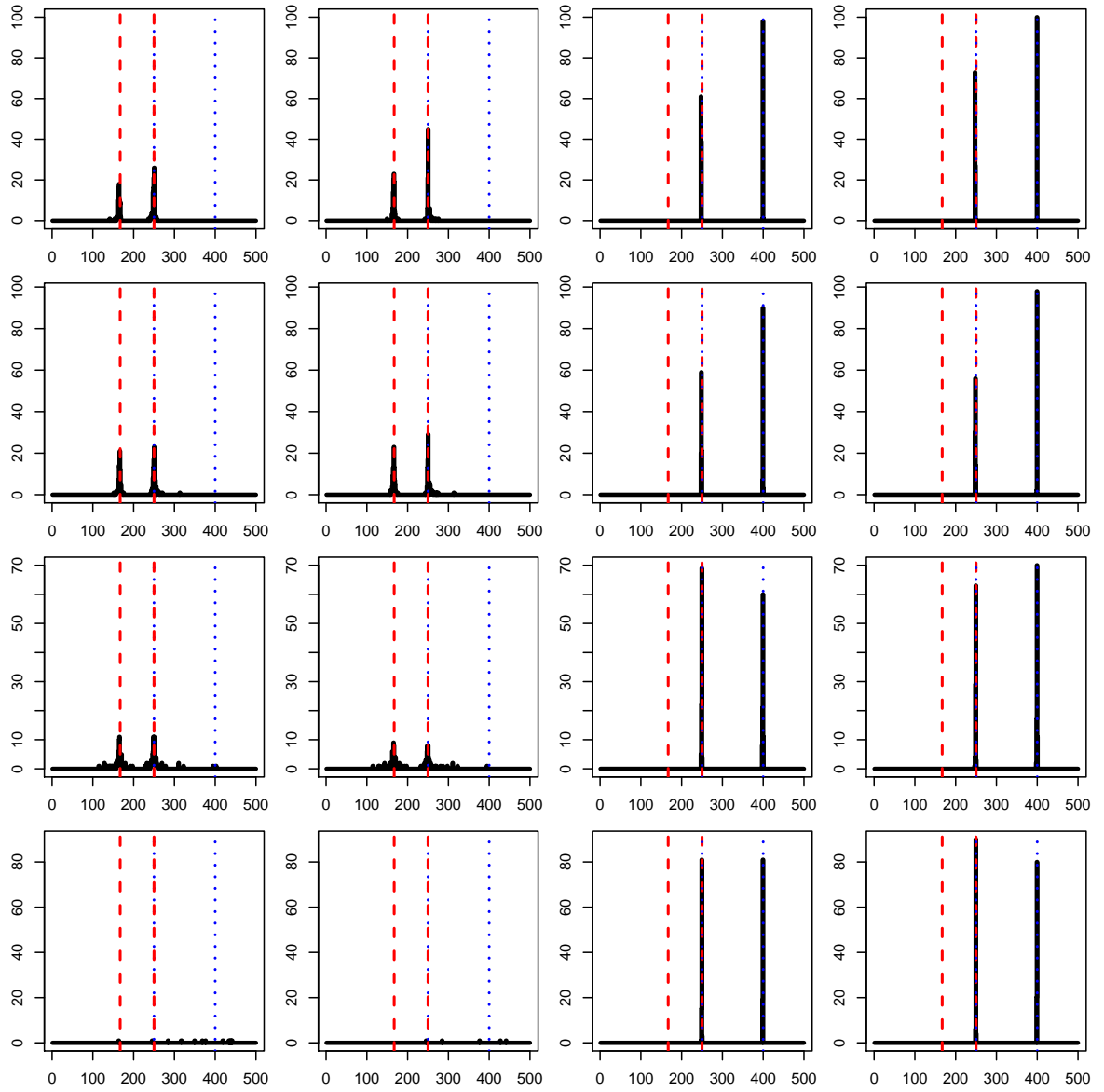


Figure 27: (M1) LOCATIONS OF THE ESTIMATED CHANGE-POINTS WHEN $n = 300$, $T = 500$ AND $\phi = 1$.

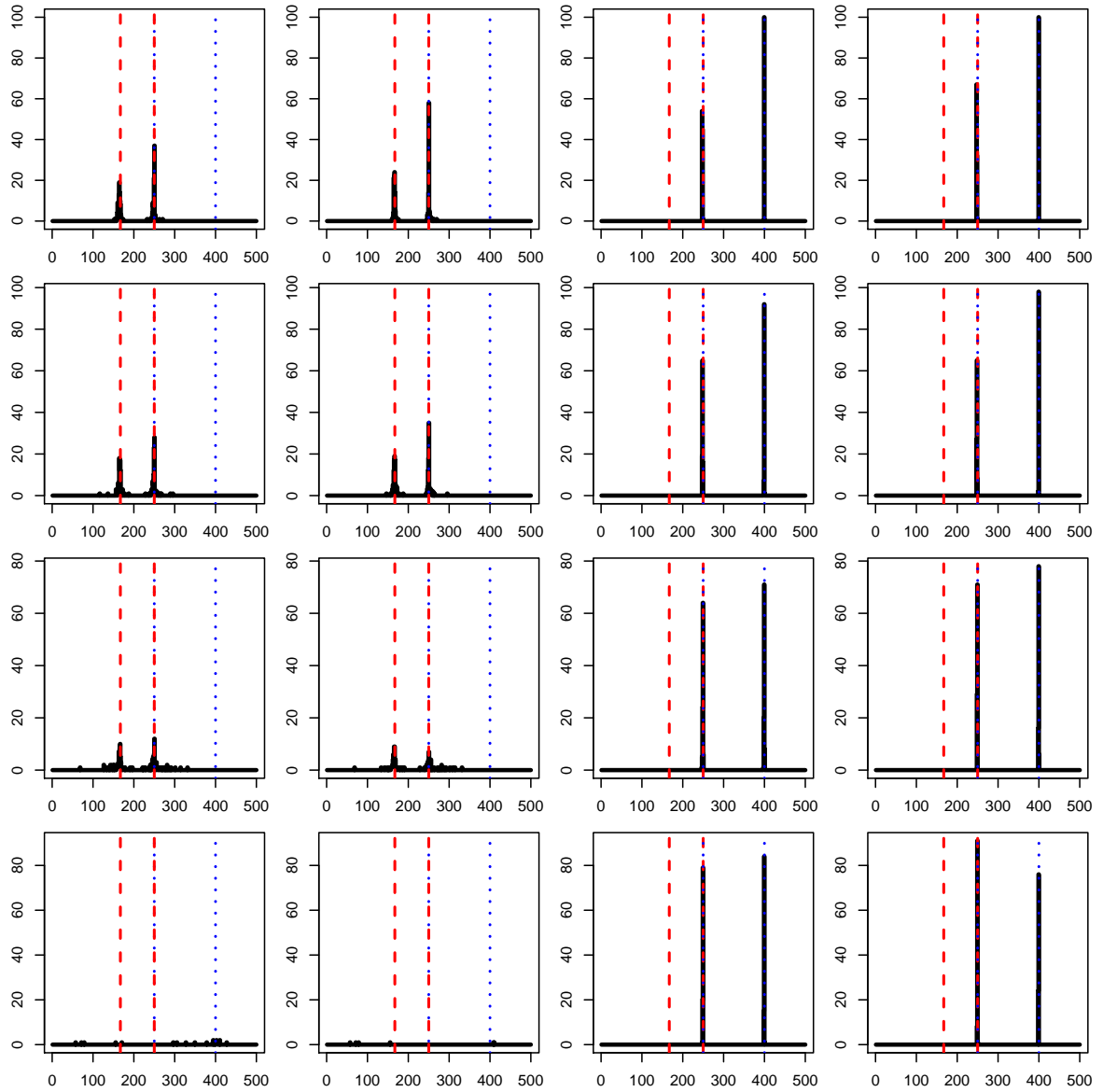


Figure 28: (M1) LOCATIONS OF THE ESTIMATED CHANGE-POINTS WHEN $n = 300$, $T = 500$ AND $\phi = 1.5$.

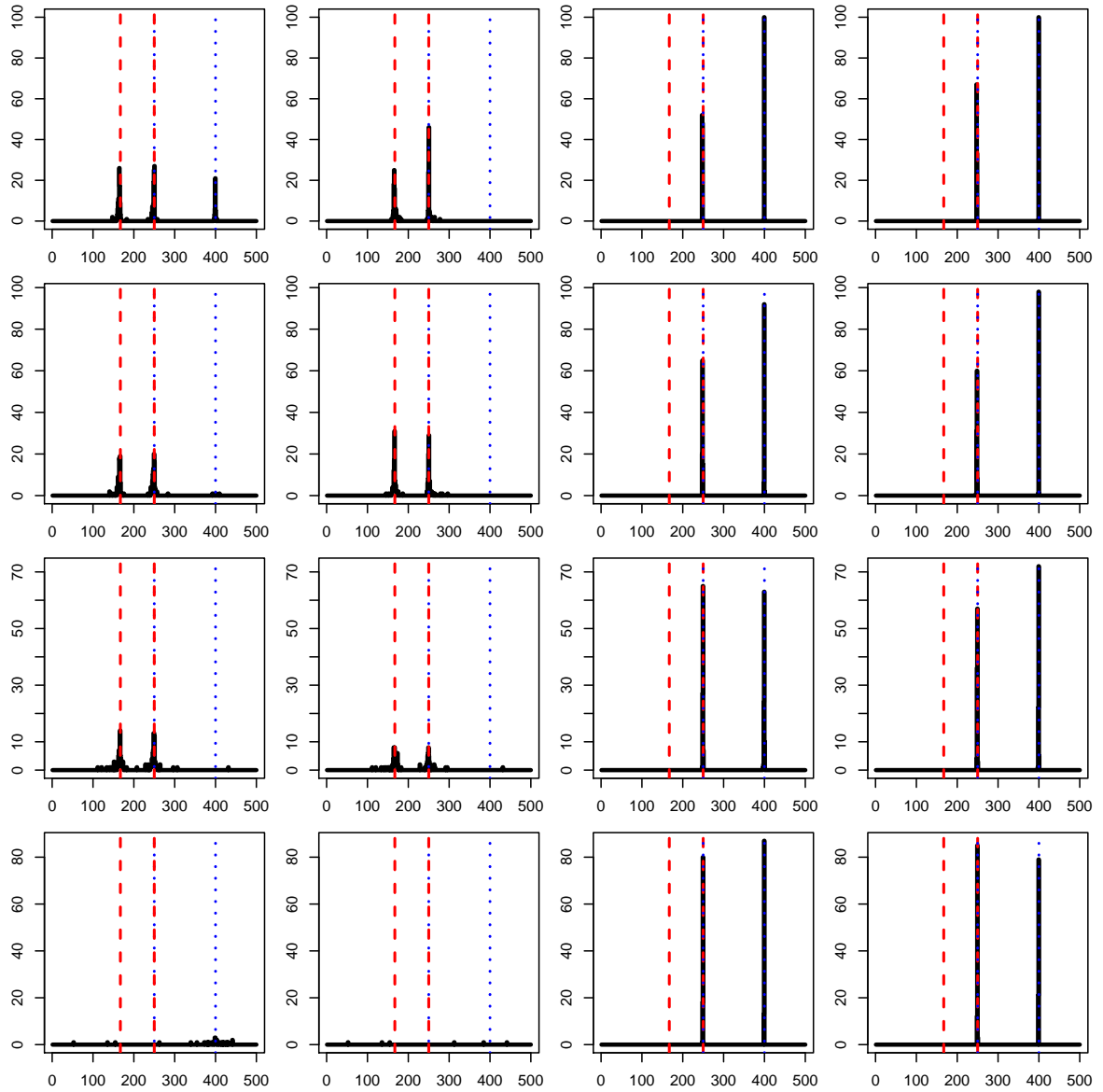


Figure 29: (M1) LOCATIONS OF THE ESTIMATED CHANGE-POINTS WHEN $n = 300$, $T = 500$ AND $\phi = 2$.

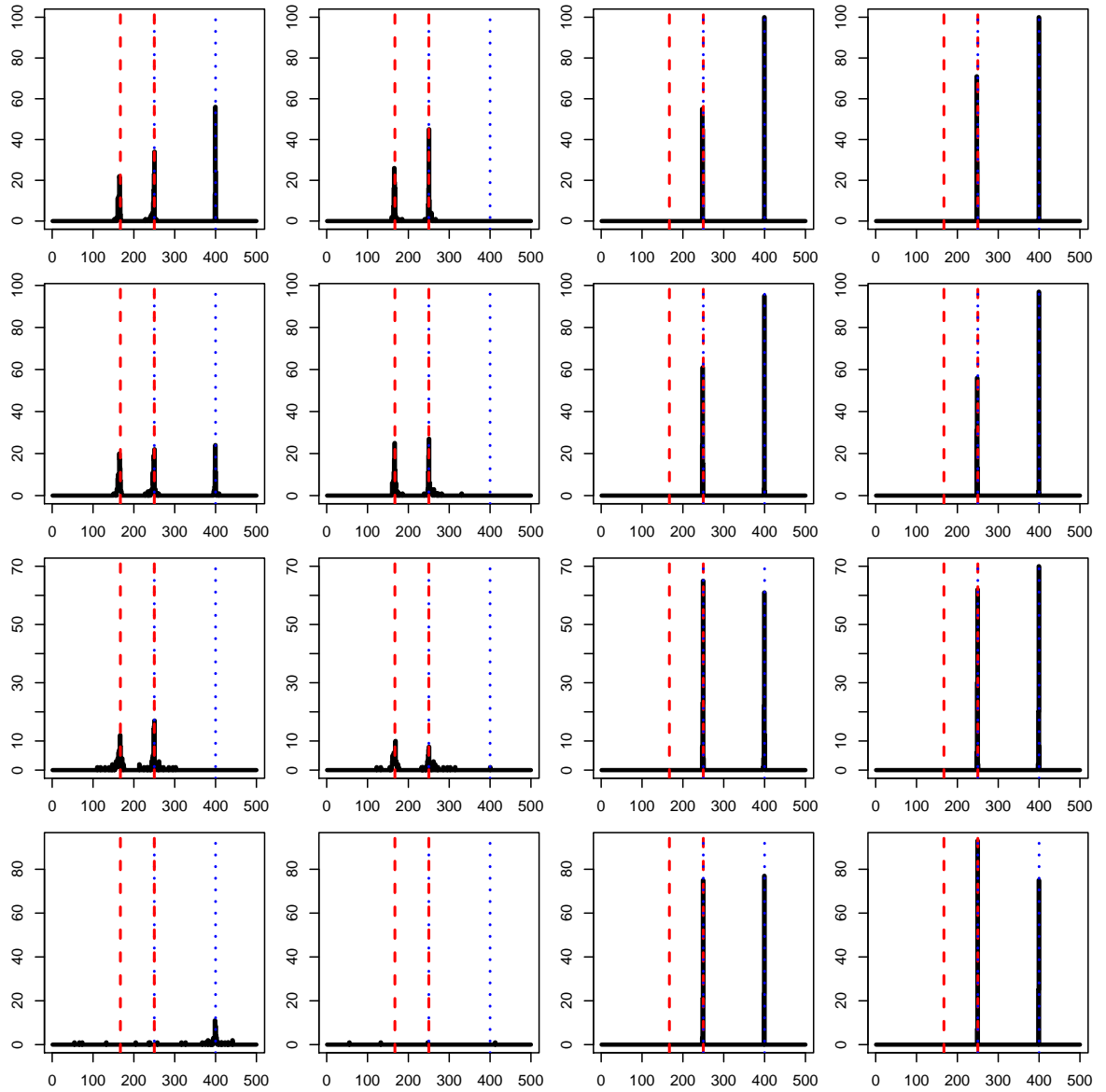


Figure 30: (M1) LOCATIONS OF THE ESTIMATED CHANGE-POINTS WHEN $n = 300$, $T = 500$ AND $\phi = 2.5$.

3.2 Additional simulation results from (M2)

Table 20: (M2) SUMMARY OF THE TOTAL NUMBER AND LOCATION ACCURACY ($|\widehat{\eta}_b - \eta_b| < 2 \log T$ in %) OF THE ESTIMATED CHANGE-POINTS WHEN $n = 100$, $T = 500$ AND $\sigma = \sqrt{2}$.

ϕ	ϱ	$\widehat{\chi}_{it}^*$						$\widehat{\epsilon}_{it}^*$						ϵ_{it}			
		avg(\widehat{B}_X)	sd(\widehat{B}_X)	η_1^χ	η_2^χ	η_3^χ	avg(\widehat{B}_X)	sd(\widehat{B}_X)	η_1^χ	η_2^χ	η_3^χ	avg(\widehat{B}_ϵ)	sd(\widehat{B}_ϵ)	η_1^ϵ	avg(\widehat{B}_ϵ)	sd(\widehat{B}_ϵ)	η_1^ϵ
1	1	2.88	0.41	99	91	59	2.85	0.36	99	90	60	1.11	0.31	100	1.07	0.29	100
	0.75	2.96	0.35	99	87	68	2.95	0.33	98	92	76	1.16	0.37	100	1.09	0.29	100
	0.5	2.91	0.51	98	95	54	2.89	0.47	100	96	69	1.22	0.54	100	1.09	0.29	100
	0.25	2.50	0.56	91	91	26	2.57	0.57	92	97	38	1.16	0.39	82	1.04	0.20	100
1.5	1	2.81	0.44	100	90	45	2.87	0.39	100	93	52	1.07	0.26	100	1.12	0.36	100
	0.75	2.88	0.38	98	97	59	2.89	0.35	98	96	72	1.13	0.37	100	1.08	0.27	100
	0.5	2.82	0.50	99	94	52	2.91	0.40	99	97	69	1.08	0.27	100	1.05	0.22	100
	0.25	2.48	0.66	84	90	20	2.74	0.58	95	91	45	1.16	0.39	83	1.07	0.26	100
2	1	2.76	0.45	100	88	40	2.83	0.38	100	87	55	1.17	0.38	99	1.14	0.35	100
	0.75	2.84	0.42	99	86	50	2.89	0.35	99	93	63	1.06	0.24	100	1.14	0.35	100
	0.5	2.77	0.57	93	84	41	3.02	0.40	97	89	65	1.10	0.30	100	1.07	0.33	100
	0.25	2.32	0.51	75	89	6	2.66	0.62	94	94	44	1.11	0.31	87	1.08	0.27	99
2.5	1	2.75	0.46	100	90	44	2.83	0.38	100	95	56	1.05	0.22	100	1.11	0.31	100
	0.75	2.70	0.46	98	89	39	2.94	0.28	99	92	72	1.06	0.24	100	1.10	0.30	100
	0.5	2.53	0.54	92	83	22	2.94	0.49	99	91	59	1.12	0.33	99	1.11	0.31	100
	0.25	2.19	0.44	74	84	4	2.76	0.61	97	92	43	1.16	0.39	82	1.05	0.22	100

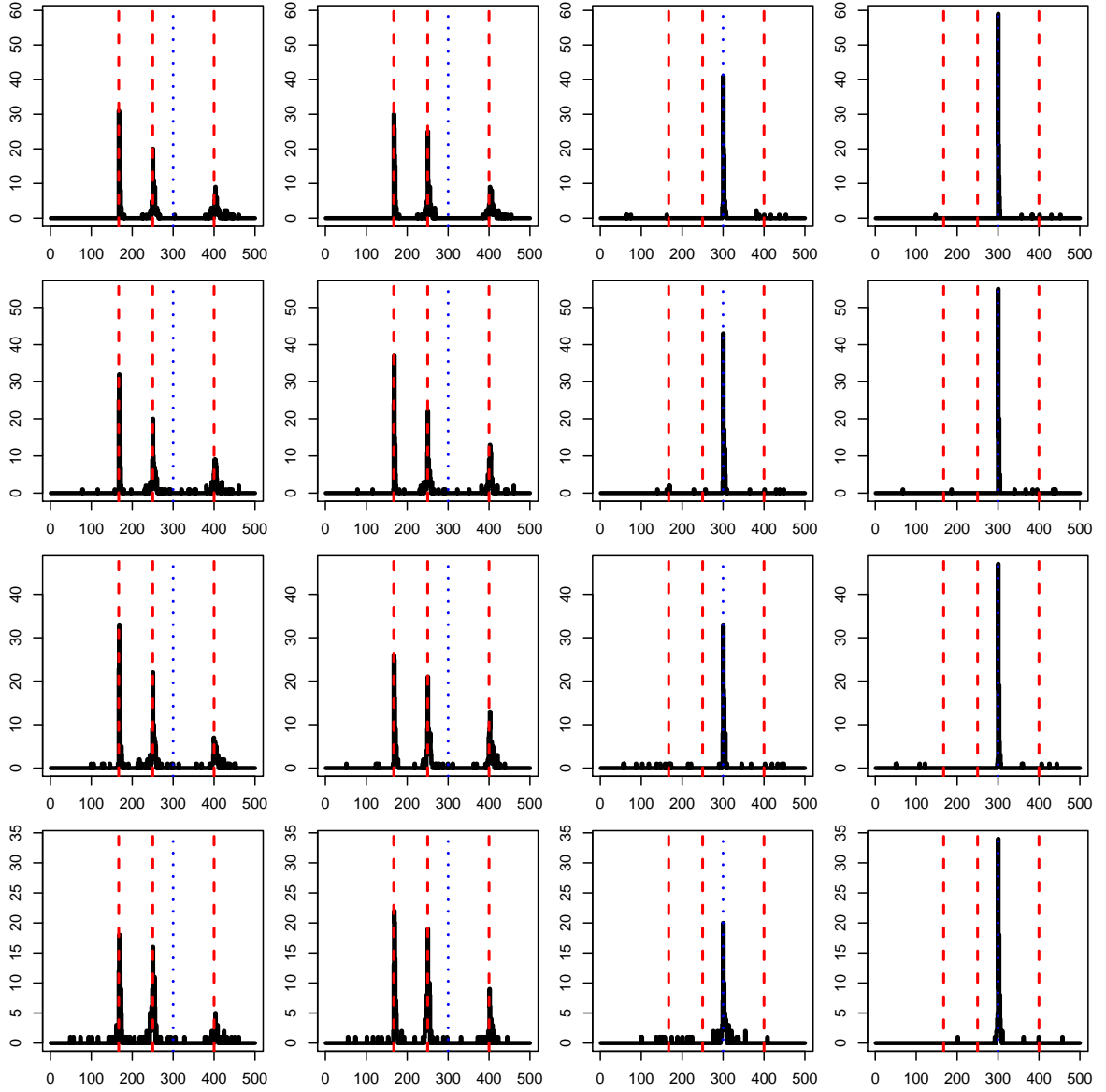


Figure 31: (M2) LOCATIONS OF THE CHANGE-POINTS ESTIMATED FROM $\hat{\chi}_{it}^*$, χ_{it} (ORACLE), $\hat{\epsilon}_{it}^*$ AND ϵ_{it} (ORACLE) BY THE DCBS ALGORITHM (LEFT TO RIGHT) FOR $\varrho \in \{1, 0.75, 0.5, 0.25\}$ (TOP TO BOTTOM) WHEN $n = 100$, $T = 500$, $\sigma = \sqrt{2}$ AND $\phi = 1$; VERTICAL LINES INDICATE THE LOCATIONS OF THE TRUE CHANGE-POINTS η_b^χ , $b = 1, 2, 3$ (BROKEN) AND η_1^ϵ (DOTTED).

References

- Bai, J. and Ng, S. (2002), “Determining the number of factors in approximate factor models,” *Econometrica*, 70, 191–221.
- Barigozzi, M., Cho, H., and Fryzlewicz, P. (2018), “Simultaneous multiple change-

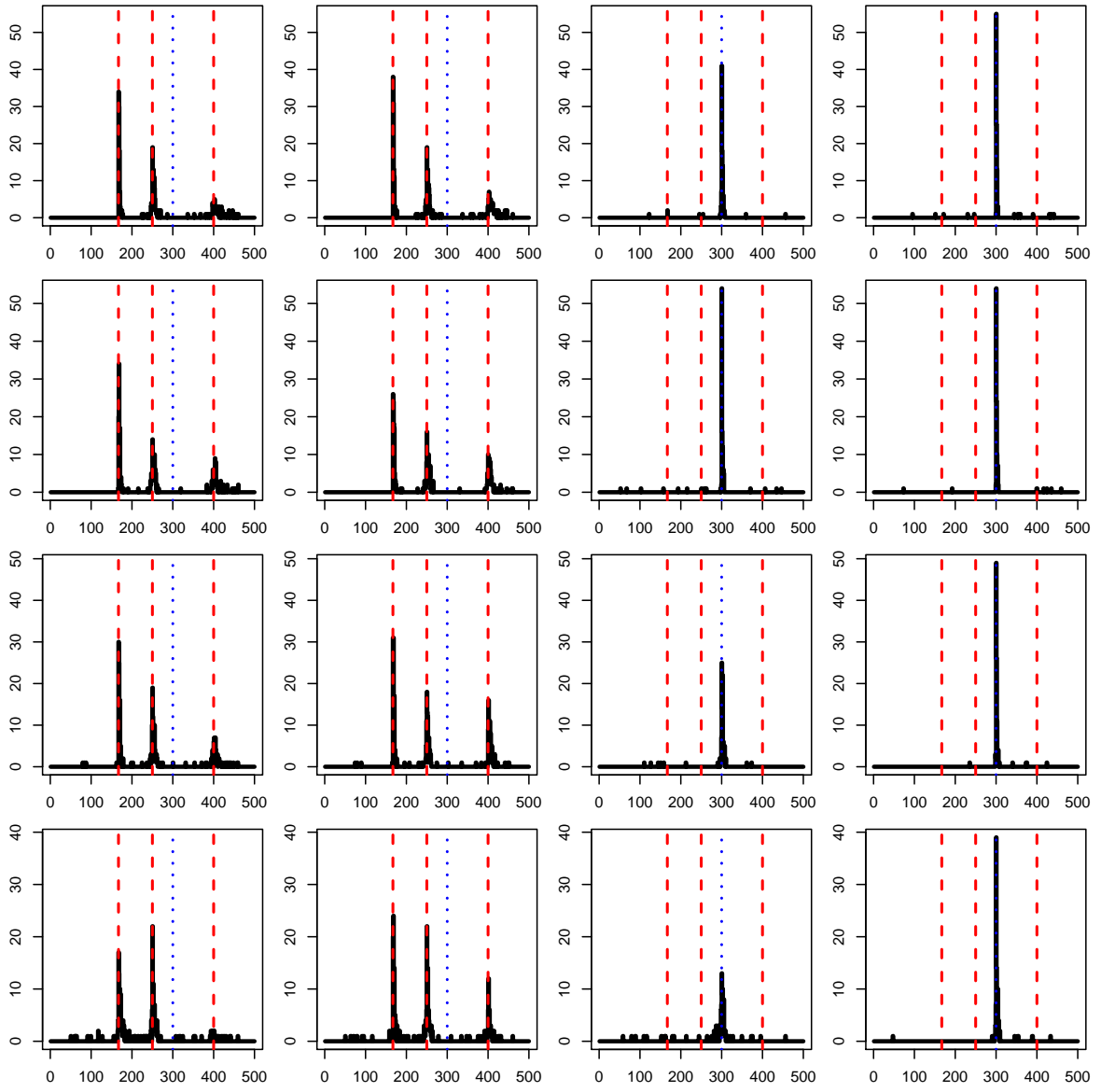


Figure 32: (M2) LOCATIONS OF THE ESTIMATED CHANGE-POINTS WHEN $n = 100$, $T = 500$, $\sigma = \sqrt{2}$ AND $\phi = 1.5$.

point and factor analysis for high-dimensional time series,” Tech. rep., arXiv preprint, arXiv:1612.06928.

Chen, L., Dolado, J. J., and Gonzalo, J. (2014), “Detecting big structural breaks in large factor models,” *Journal of Econometrics*, 180, 30–48.

Han, X. and Inoue, A. (2014), “Tests for parameter instability in dynamic factor models,” *Econometric Theory*, 31, 1–36.

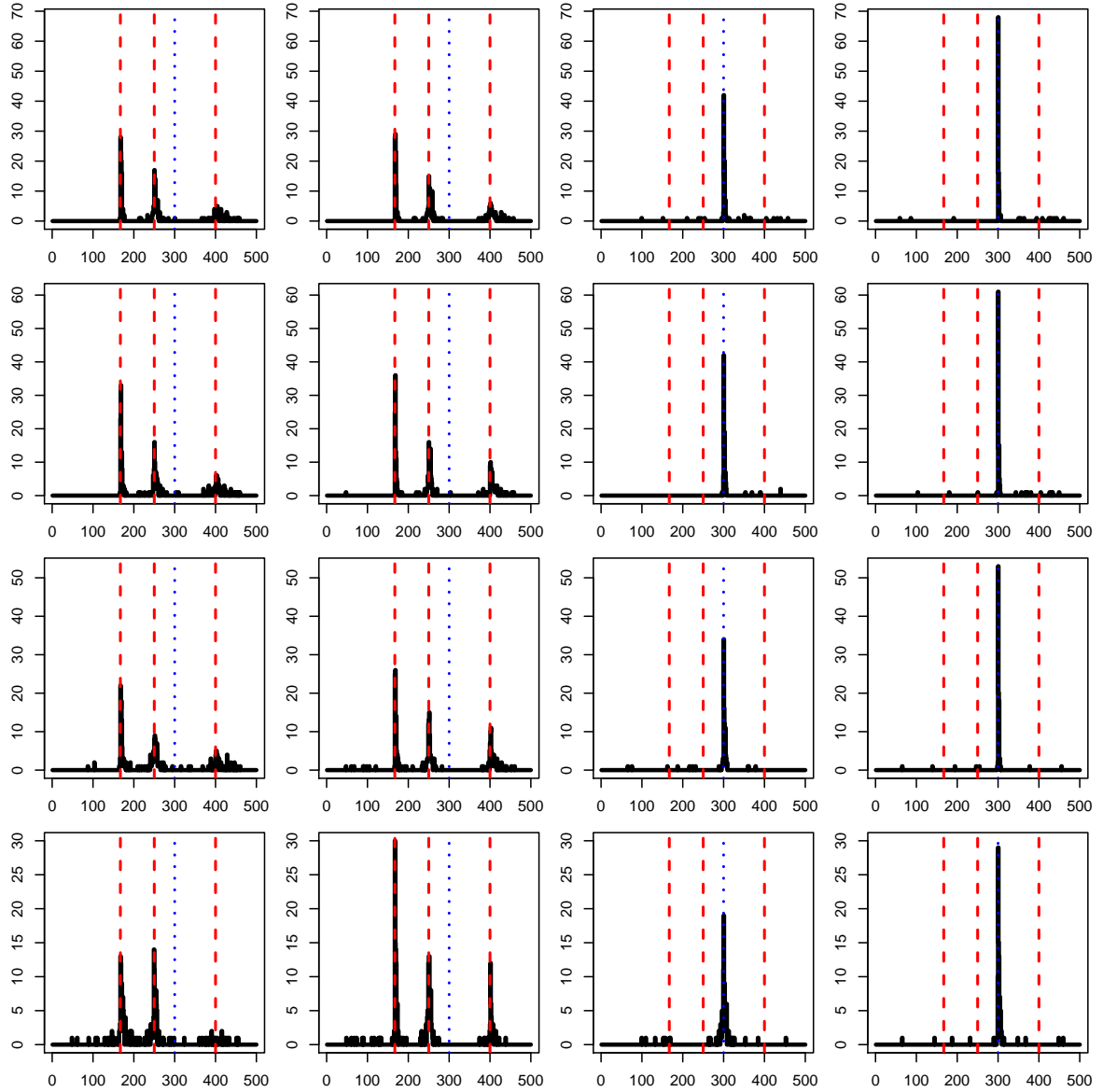


Figure 33: (M2) LOCATIONS OF THE ESTIMATED CHANGE-POINTS WHEN $n = 100$, $T = 500$, $\sigma = \sqrt{2}$ AND $\phi = 2$.

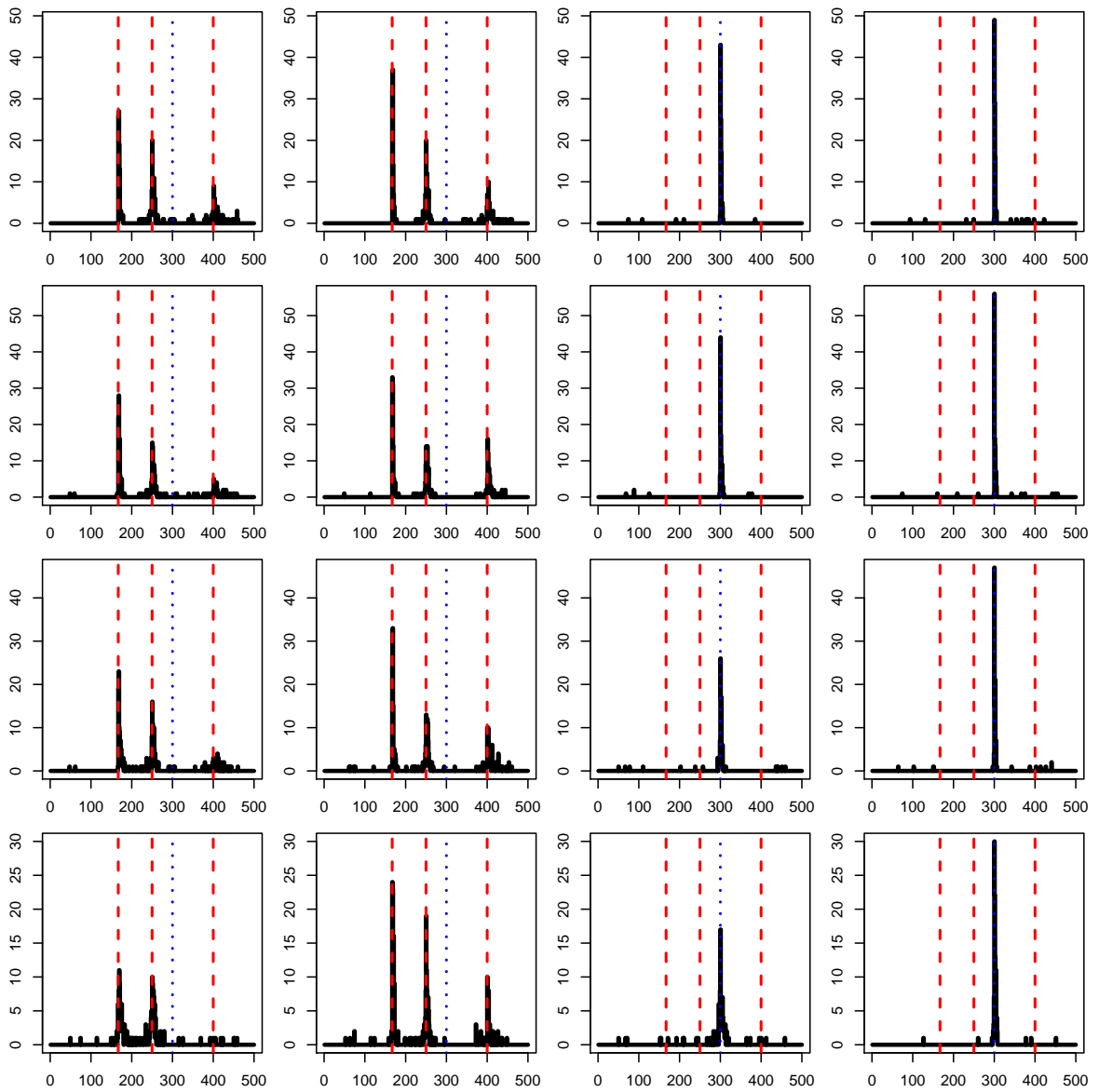


Figure 34: (M2) LOCATIONS OF THE ESTIMATED CHANGE-POINTS WHEN $n = 100$, $T = 500$, $\sigma = \sqrt{2}$ AND $\phi = 2.5$.

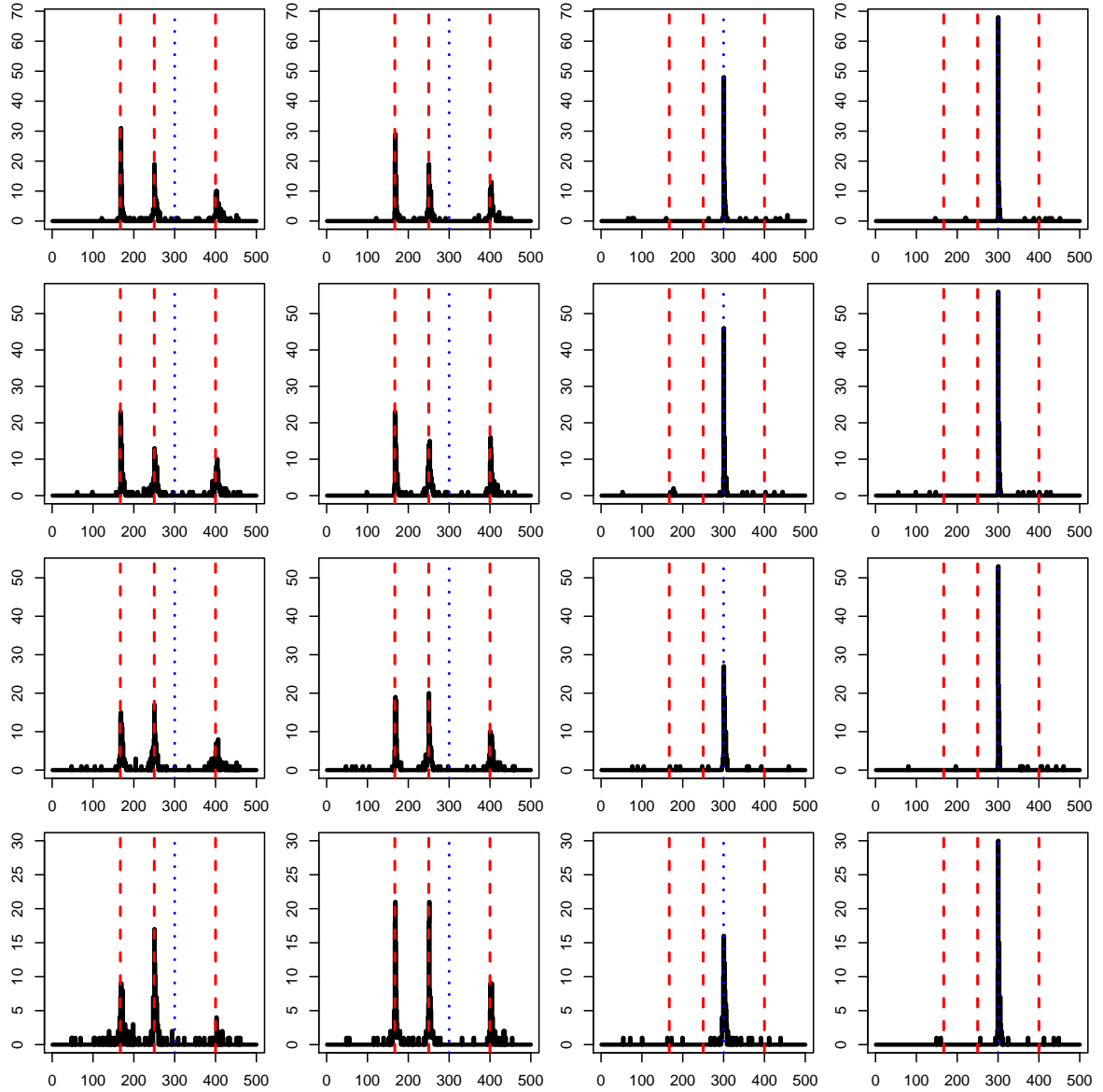


Figure 35: (M2) LOCATIONS OF THE ESTIMATED CHANGE-POINTS WHEN $n = 100$, $T = 500$, $\sigma = 0.75\sqrt{2}$ AND $\phi = 1.5$.

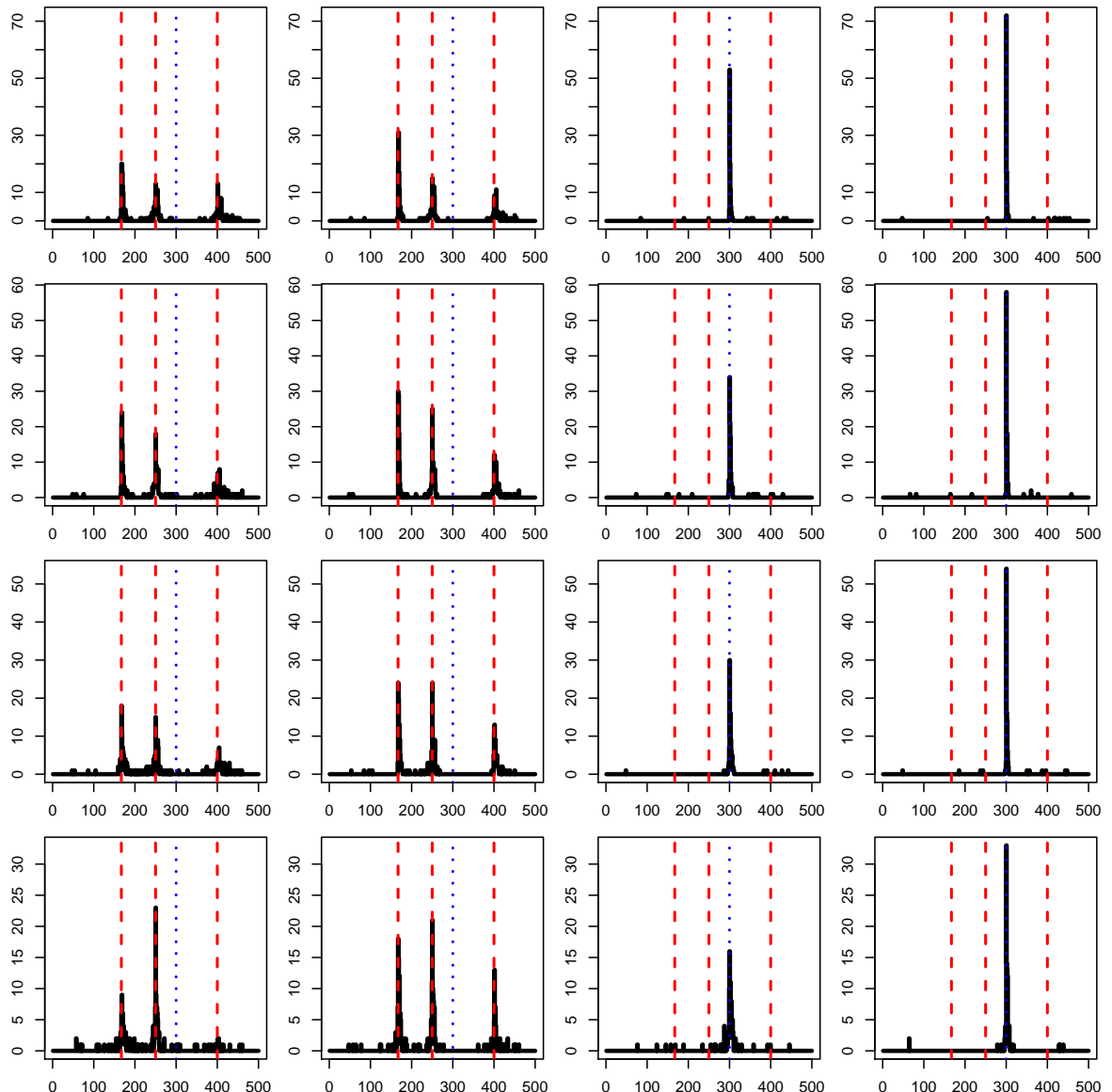


Figure 36: (M2) LOCATIONS OF THE ESTIMATED CHANGE-POINTS WHEN $n = 100$, $T = 500$, $\sigma = 0.75\sqrt{2}$ AND $\phi = 2$.

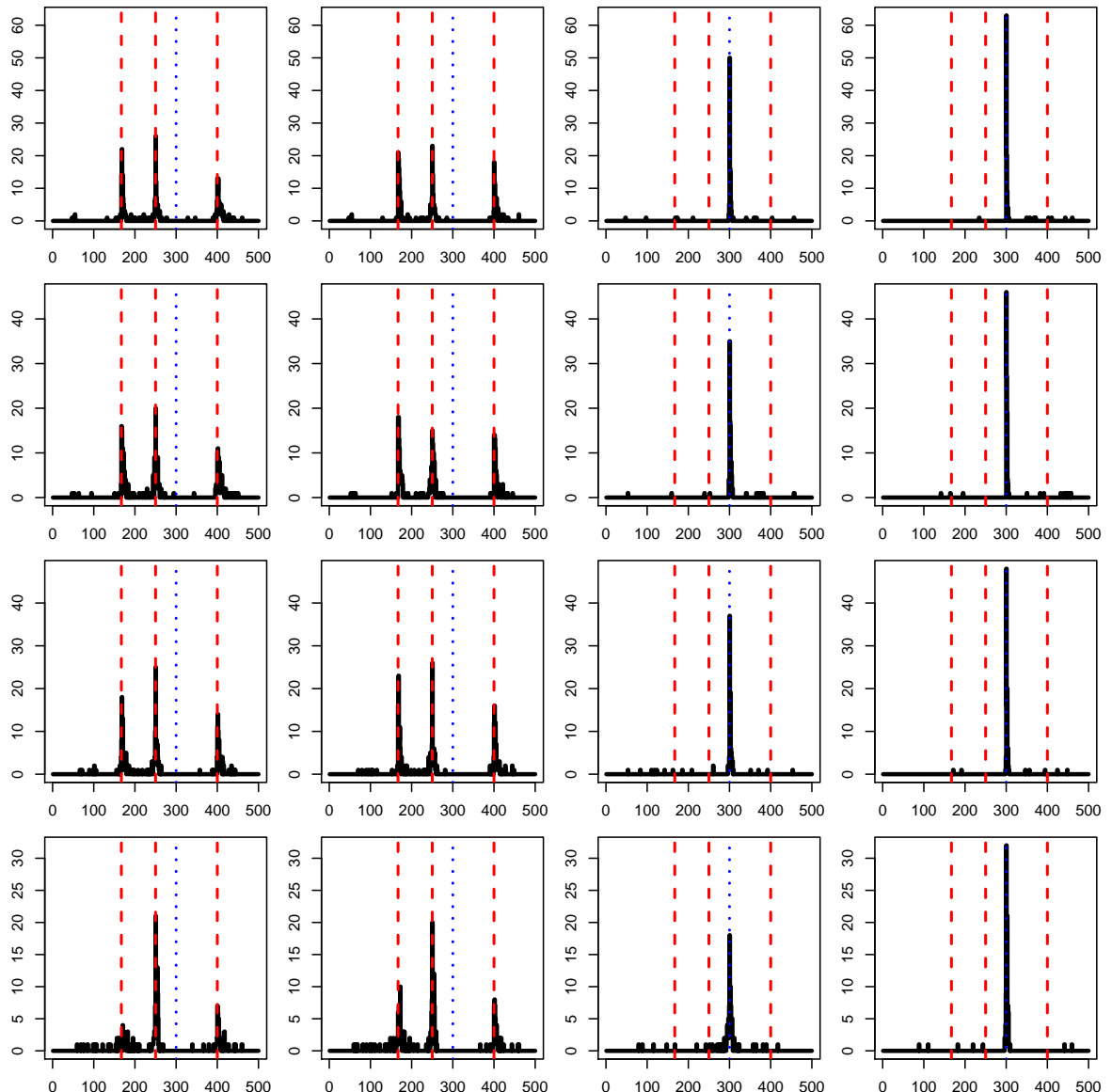


Figure 37: (M2) LOCATIONS OF THE ESTIMATED CHANGE-POINTS WHEN $n = 100$, $T = 500$, $\sigma = 0.5\sqrt{2}$ AND $\phi = 1$.

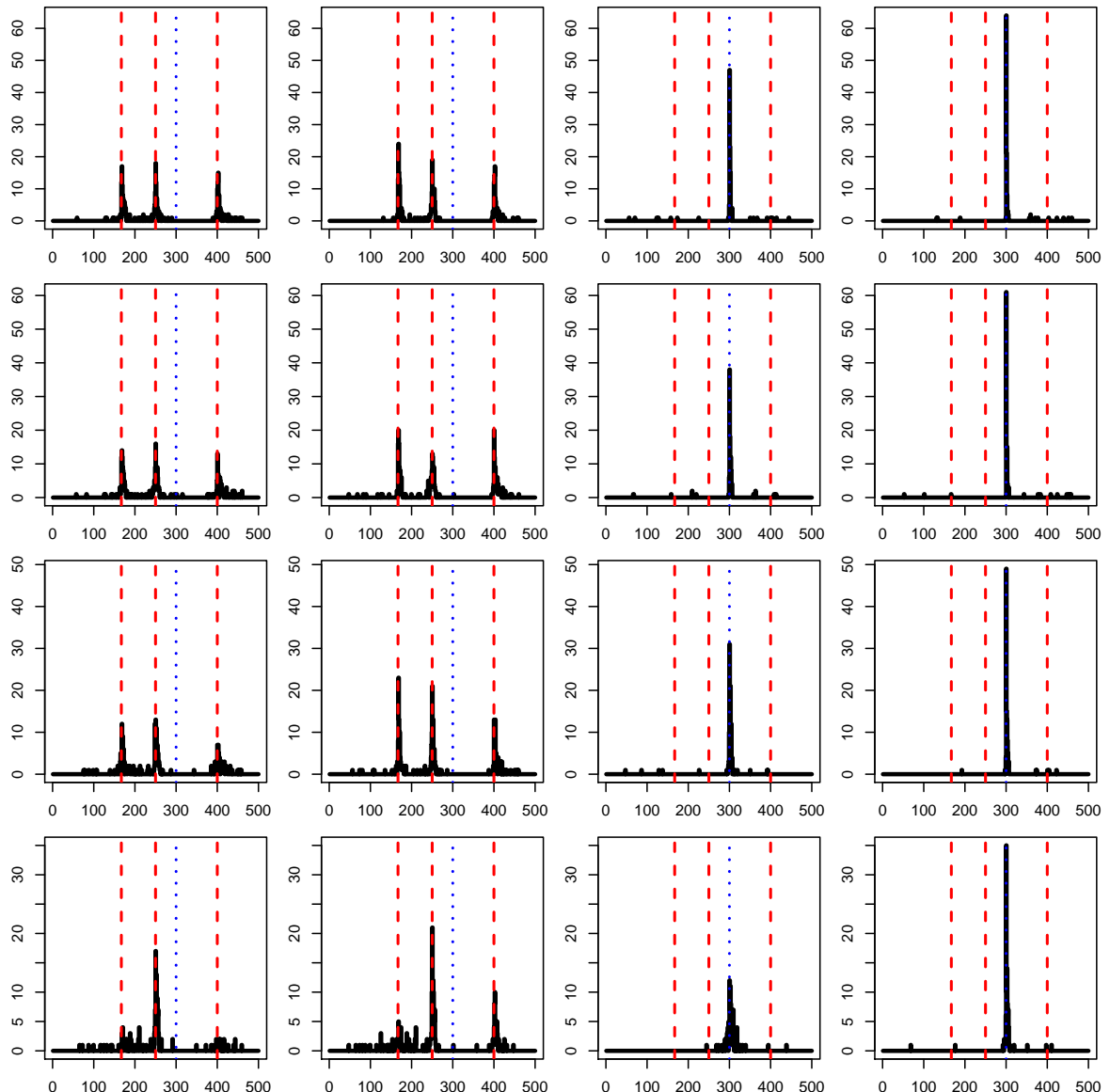


Figure 38: (M2) LOCATIONS OF THE ESTIMATED CHANGE-POINTS WHEN $n = 100$, $T = 500$, $\sigma = 0.5\sqrt{2}$ AND $\phi = 1.5$.

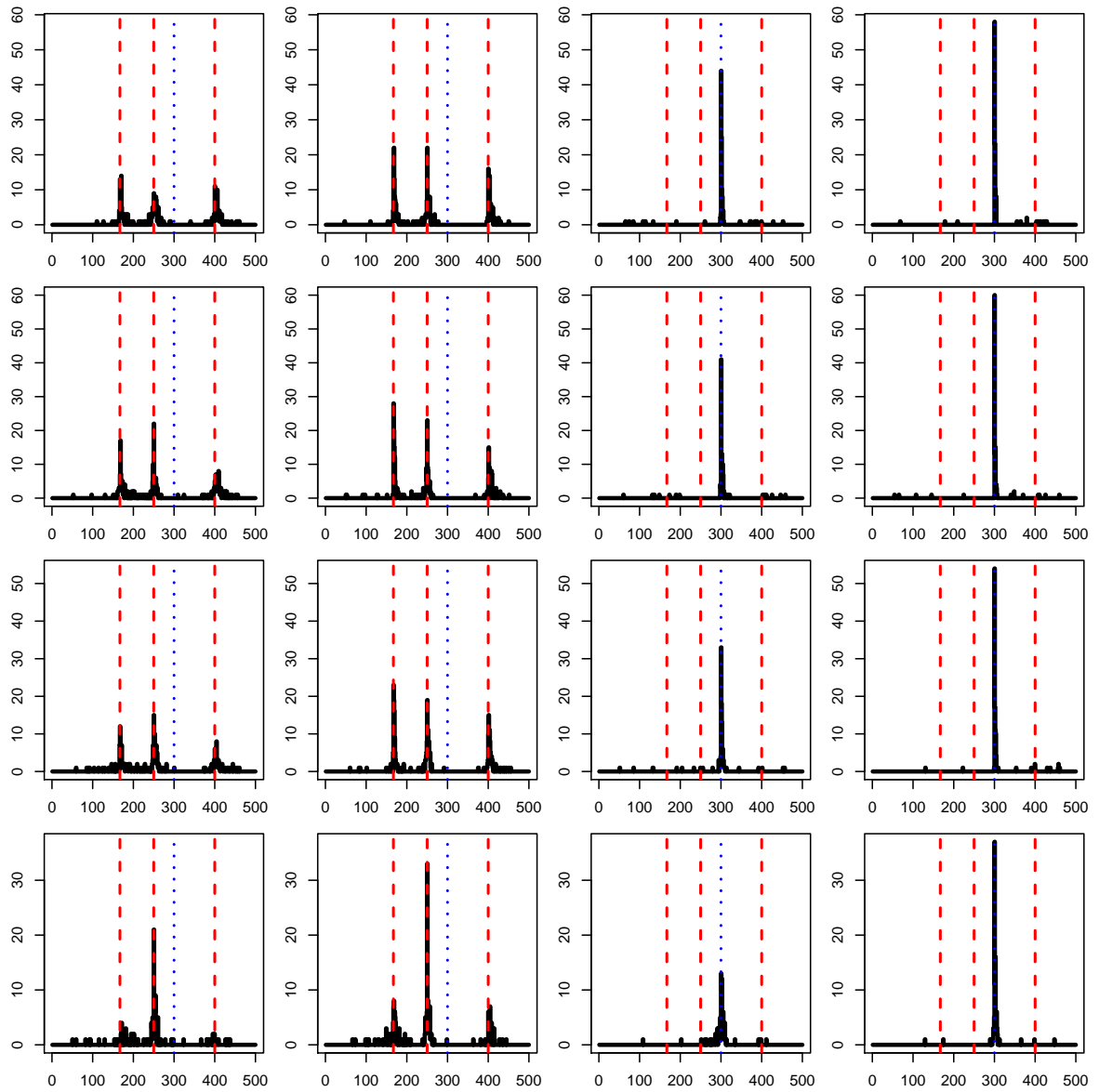


Figure 39: (M2) LOCATIONS OF THE ESTIMATED CHANGE-POINTS WHEN $n = 100$, $T = 500$, $\sigma = 0.5\sqrt{2}$ AND $\phi = 2$.

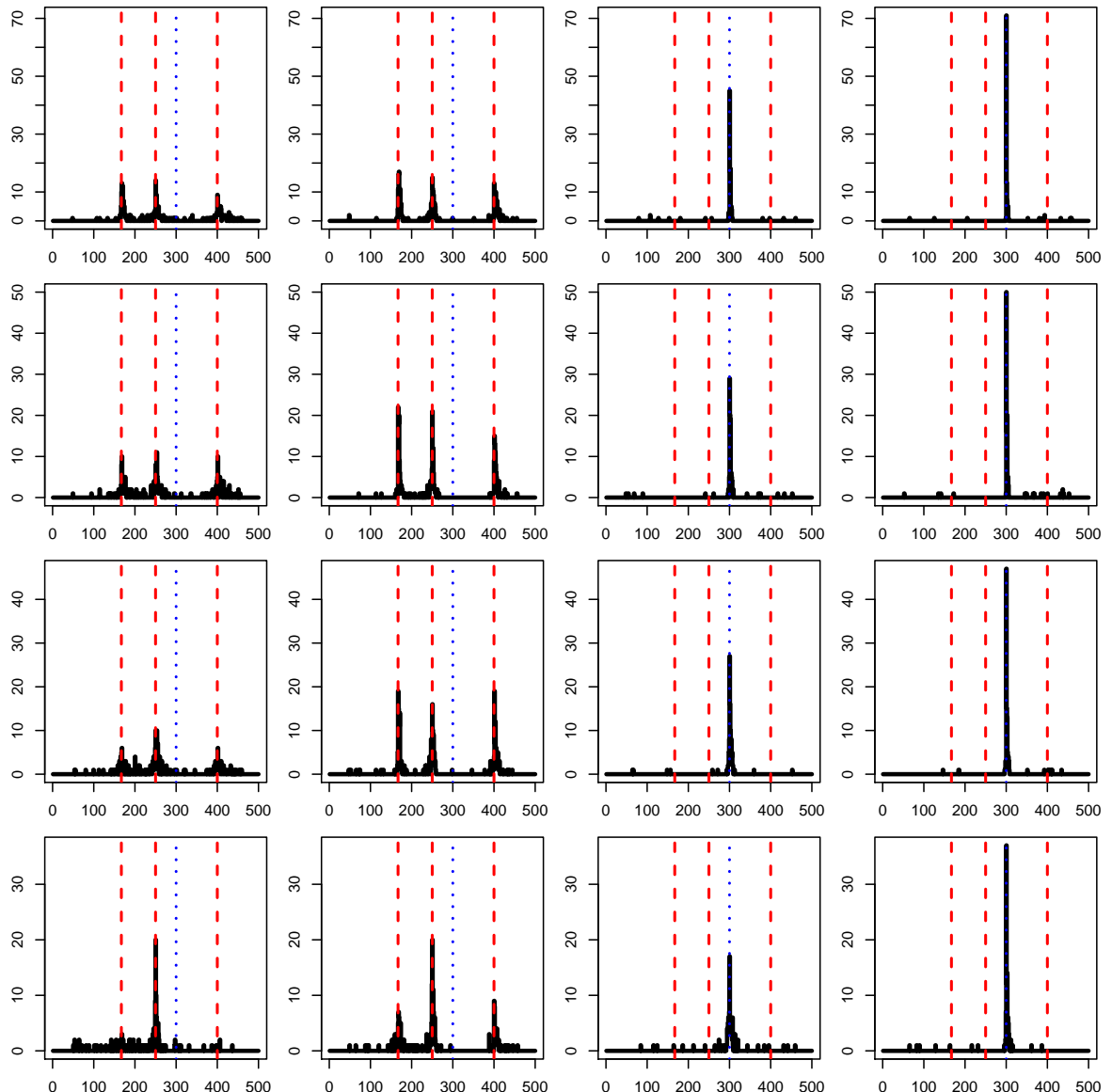


Figure 40: (M2) LOCATIONS OF THE ESTIMATED CHANGE-POINTS WHEN $n = 100$, $T = 500$, $\sigma = 0.5\sqrt{2}$ AND $\phi = 2.5$.

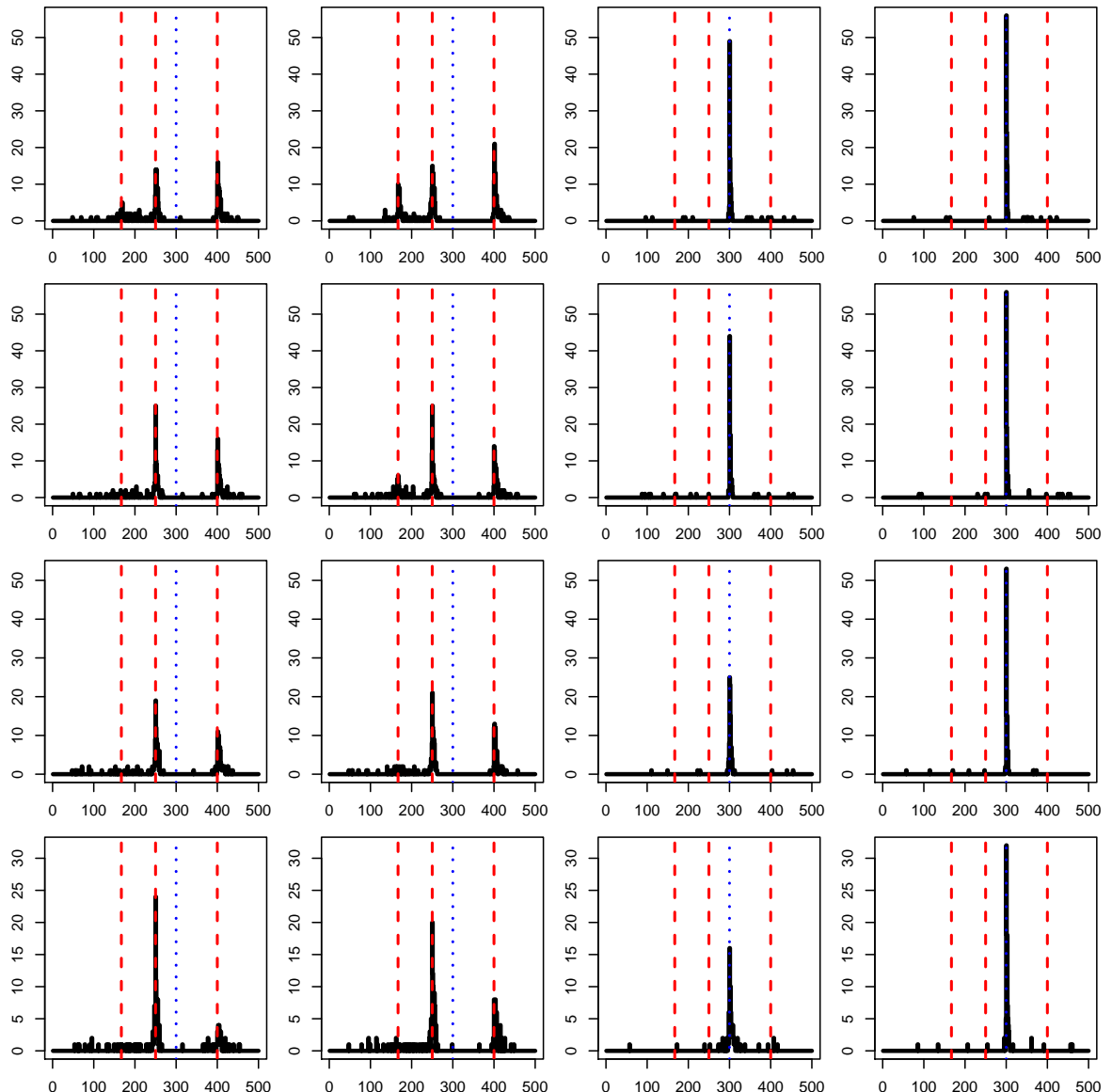


Figure 41: (M2) LOCATIONS OF THE ESTIMATED CHANGE-POINTS WHEN $n = 100$, $T = 500$, $\sigma = 0.25\sqrt{2}$ AND $\phi = 1$.

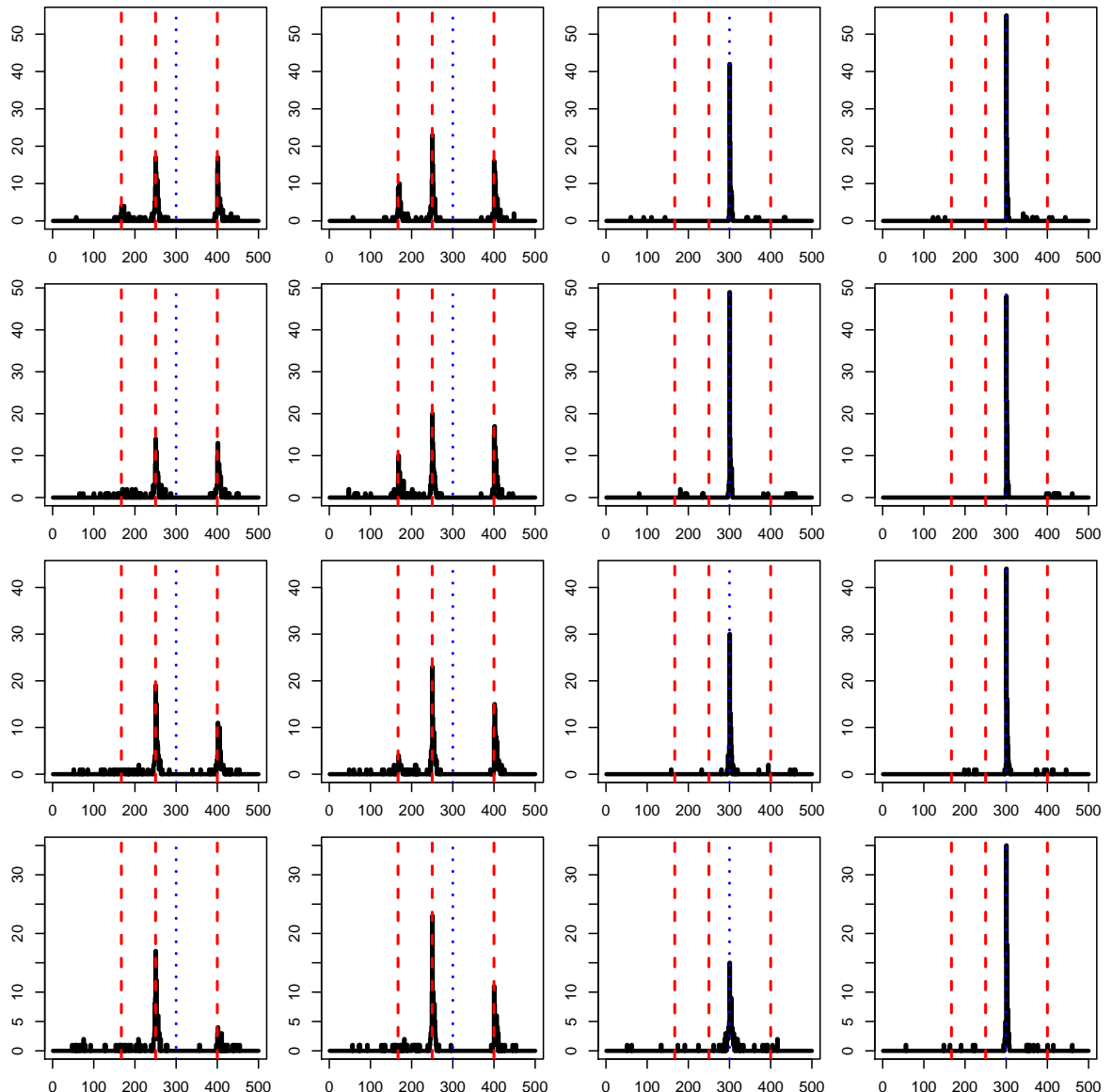


Figure 42: (M2) LOCATIONS OF THE ESTIMATED CHANGE-POINTS WHEN $n = 100$, $T = 500$, $\sigma = 0.25\sqrt{2}$ AND $\phi = 1.5$.

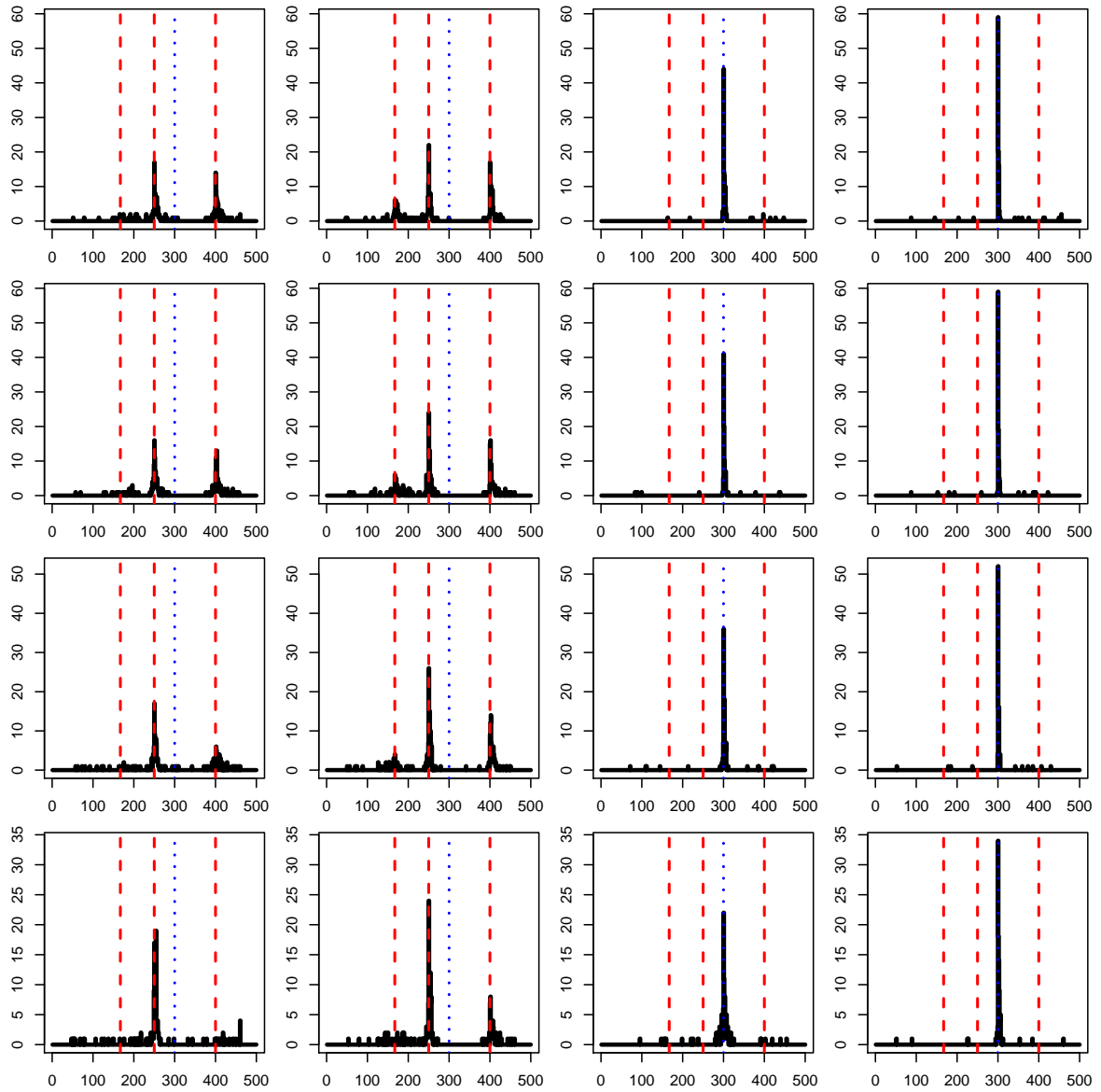


Figure 43: (M2) LOCATIONS OF THE ESTIMATED CHANGE-POINTS WHEN $n = 100$, $T = 500$, $\sigma = 0.25\sqrt{2}$ AND $\phi = 2$.

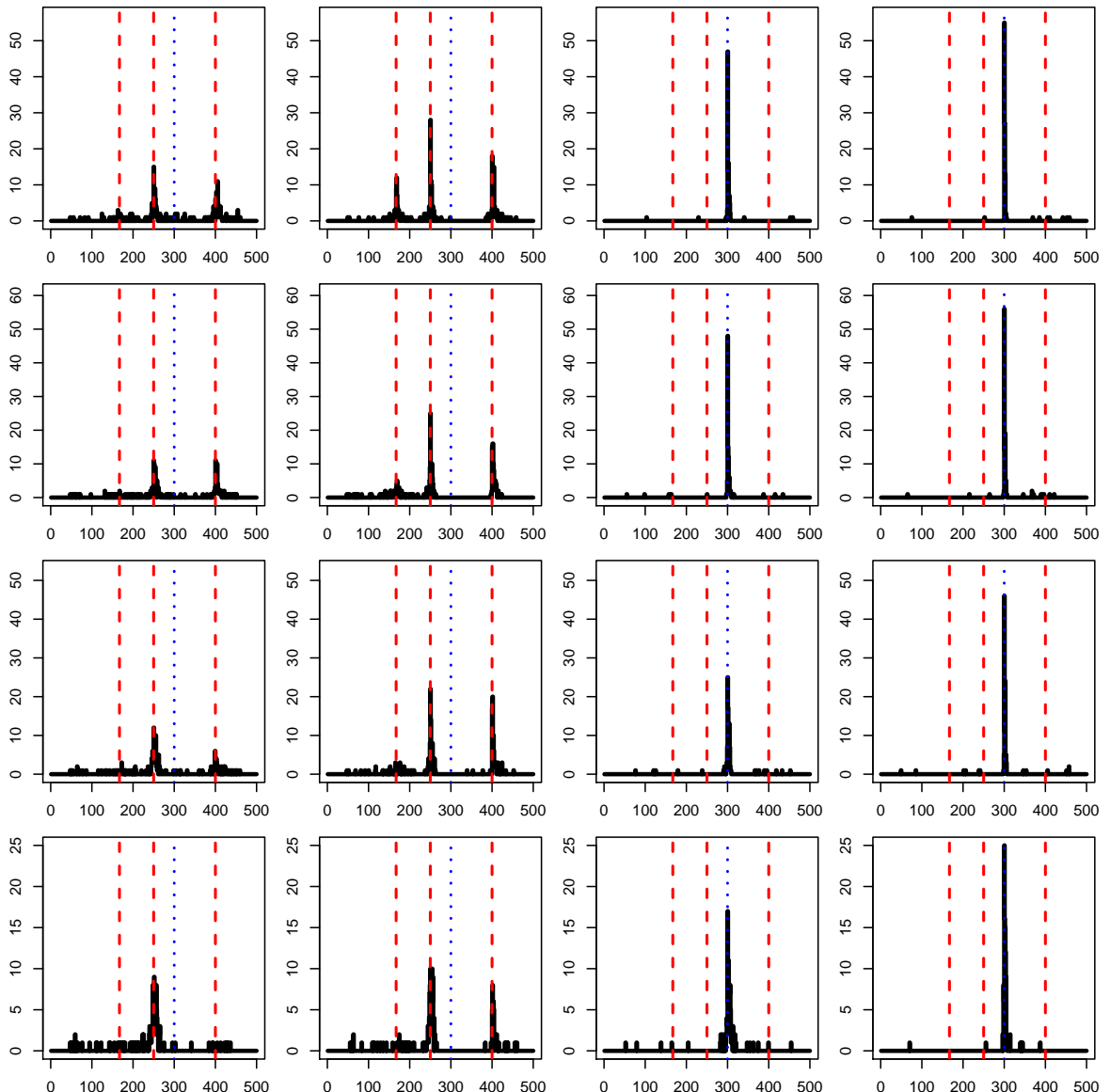


Figure 44: (M2) LOCATIONS OF THE ESTIMATED CHANGE-POINTS WHEN $n = 100$, $T = 500$, $\sigma = 0.25\sqrt{2}$ AND $\phi = 2.5$.